A chemical screen based on an interruption of zebrafish gastrulation identifies the HTR2C inhibitor Pizotifen as a suppressor of EMT-mediated metastasis

Joji Nakayama[1,2,3,4,§], Lora Tan[1], Boon Cher Goh[2], Shu Wang[1, 5], Hideki Makinoshima[3,6] and Zhiyuan Gong[1,§]

[1]Department of Biological Science, National University of Singapore, Singapore
[2]Cancer Science Institute of Singapore, National University of Singapore, Singapore
[3]Tsuruoka Metabolomics Laboratory, National Cancer Center, Tsuruoka, Japan
[4]Shonai Regional Industry Promotion Center, Tsuruoka, Japan.
[5]Institute of Bioengineering and Nanotechnology, Singapore
[6]Division of Translational Research, Exploratory Oncology Research and Clinical Trial Center, National Cancer Center, Kashiwa, Japan.

[§]Corresponding authors:
Joji Nakayama
email: Zmetastasis@gmail.com

Zhiyuan Gong
email: dbsgzy@nus.edu.sg

Keywords: Metastasis, gastrulation, EMT, Phenotyping screening, zebrafish

Total words excluding supplemental figure legends and references section: 5468

Number of figures: 5
Number of tables: 1
Number of supplemental figures: 3
Number of supplemental tables: 2

Abstract

Metastasis is responsible for approximately 90% of cancer-associated mortality but few models exist that allow for rapid and effective screening of anti-metastasis drugs. Current mouse models of metastasis are too expensive and time consuming to use for rapid and high-throughput screening. Therefore, we created a unique screening concept utilizing conserved mechanisms between zebrafish gastrulation and cancer metastasis for identification of potential anti-metastatic drugs. We hypothesized that small chemicals that interrupt zebrafish gastrulation might also suppress metastatic progression of cancer cells and developed a phenotype-based chemical screen to test the hypothesis. The screen used epiboly, the first morphogenetic movement in gastrulation, as a marker and enabled 100 chemicals to be tested in five hours. The screen tested 1280 FDA-approved drugs and identified Pizotifen, an antagonist for serotonin receptor 2C (HTR2C) as an epiboly-interrupting drug. Pharmacologic and genetic inhibition of HTR2C suppressed metastatic progression in a mouse model. Blocking HTR2C with Pizotifen restored epithelial properties to metastatic cells through inhibition of Wnt-signaling. In contrast, HTR2C induced epithelial to mesenchymal transition (EMT) through activation of Wnt-signaling and promoted metastatic dissemination of human cancer cells in a zebrafish xenotransplantation model. Taken together, our concept offers a novel platform for discovery of anti-metastasis drugs.

Introduction

Metastasis, a leading contributor to the morbidity of cancer patients, occurs through multiple steps: invasion, intravasation, extravasation, colonization, and metastatic tumor formation (1-3). The physical translocation of cancer cells is an initial step of metastasis and molecular mechanisms of it involve cell motility, the breakdown of local basement membrane, loss of cell polarity, acquisition of stem cell-like properties, and EMT (4-6). These cell-biological phenomena are also observed during vertebrate gastrulation in that evolutionarily conserved morphogenetic movements of epiboly, internalization, convergence, and extension progress (7). In zebrafish, the first morphogenetic movement, epiboly, is initiated at approximately 4 hours post fertilization (hpf) to move cells from the animal pole to eventually engulf the entire yolk cell by 10 hpf (8, 9). The embryonic cell movements are governed by the molecular mechanisms that are partially shared in metastatic cell dissemination.

At least fifty common genes were shown to be involved in both metastasis and gastrulation progression: Knockdown of these genes in Xenopus or zebrafish induced gastrulation defects; conversely, overexpression of these genes conferred metastatic potential on cancer cells and knockdown of these genes suppressed metastasis (Table S1). This evidence led us to hypothesize that small molecules that interrupt zebrafish gastrulation may suppress metastatic progression of human cancer cells.

Here we report a unique screening concept based on the hypothesis. Pizotifen, an antagonist for HTR2C, was identified from the screen as a “hit” that interrupted zebrafish gastrulation. A mouse model of metastasis confirmed pharmacological and genetic inhibition of HTR2C suppressed metastatic progression. Moreover, HTR2C induced EMT and promoted metastatic dissemination of non-metastatic cancer cells in a zebrafish xenotransplantation model. These results demonstrated that this concept could offer a novel high-throughput platform for discovery of anti-metastasis drugs and can be converted to a chemical genetic screening platform.

Results

Small molecules interrupting epiboly of zebrafish have a potential to suppress metastatic progression of human cancer cells.

Before performing a screening assay, we conducted preliminary experiments to test the hypothesis. First, we examined whether hindering the molecular function of reported genes, whose knockdown induced gastrulation defects in zebrafish, might suppress cell motility and invasion of cancer cells. We chose protein arginine methyltransferase 1 (PRMT1) and cytochrome P450 family 11 (CYP11A1), both of whose knockdown induced gastrulation defects in zebrafish but whose involvement in metastatic progression is unclear (10, 11). Elevated expression of PRMT1 and CYP11A1 were observed in highly metastatic human breast cancer cell lines and knockdown of these genes through RNA interference suppressed the motility and invasion of MDA-MB-231 cells without affecting their viability (Figure S1A-C).

Next, we conducted an inverse examination of whether chemicals which were reported to suppress metastatic dissemination of cancer cells could interrupt epiboly progression of zebrafish embryos. Niclosamide and Vinpocetine are reported to suppress metastatic progression (12, 13) (14, 15). Either Niclosamide or Vinpocetine-treated zebrafish embryos showed complete arrest at very early stages or severe delay in epiboly progression, respectively (Figure S1D).

These results suggest that epiboly could serve as a marker for this screening assay and epiboly-interrupting drugs that are identified through this screening could have the potential to suppress metastatic progression of human cancer cells.

132 FDA-approved drugs induced delayed in epiboly of zebrafish embryos

We screened 1,280 FDA, EMA or other agencies-approved drugs (Prestwick, Inc) in our zebrafish assay. The screening showed that 0.9% (12/1280) of the drugs, including Actimycin A and Tolcapone, induced severe or complete arrest of embryonic cell

102 movement when embryos were treated with 10μM. 5.2% (66/1280) of the drugs, such as
103 Dicumarol, Racecadotril, Pizotifen and S(-) Eticlopride hydrochloride, induced either
104 delayed epiboly or interrupted epiboly of the embryos. 93.3% (1194/1280) of drugs has
105 no effect on epiboly progression of the embryos. 0.6% (8/1280) of drugs induced a toxic
106 lethality. Epiboly progression was affected more severely when embryos were treated
107 with 50μM; 1.7% (22/1280) of the drugs induced severe or complete arrest of it. 8.6%
108 (110/1280) of the drugs induced either delayed epiboly or interrupt epiboly of the
109 embryos. 4.3% (55/1280) of drugs induced a toxic lethality (Figure 1A and 1B, Table S2).
110 Among the epiboly-interrupting drugs, several drugs have already been reported to inhibit
111 metastasis-related molecular mechanisms: Adrenosterone or Zardaverine, which target
112 HSD11β1 or PDE3 and 4, respectively, are reported to inhibit EMT (16, 17);
113 Racecadotril, which targets enkephalinase, is reported to confer metastatic potential on
114 colon cancer cell (18); and Disulfiram, which targets ALDH, is reported to confer stem-
115 like properties on metastatic cancer cells (19). This evidence suggests that epiboly-
116 interrupting drugs have the potential for suppressing metastasis of human cancer cells.
117
118 **Identified drugs suppressed cell motility and invasion of human cancer cells.**
119 It has been reported that zebrafish have orthologues to 86% of 1318 human drug targets
120 (20). However, it was not known whether the epiboly-interrupting drugs could suppress
121 metastatic dissemination of human cancer cells. To test this, we subjected the 78 epiboly-
122 interrupting drugs that showed a suppressor effect on epiboly progression at a 10μM
123 concentration to *in vitro* experiments using a human cancer cell line. The experiments
124 examined whether the drugs could suppress cell motility and invasion of MDA-MB-231
125 cells through a Boyden chamber. Before conducting the experiment, we investigated
126 whether these drugs might effect viability of MDA-MB-231 cells using an MTT assay.
127 Sixteen of the 78 drugs strongly effected cell viability at concentrations less than 1μM
128 and were not used in the cell motility experiments. The remaining 62 drugs were assayed

129 in Boyden chamber motility experiments. Twenty of the 62 drugs inhibited cell motility
130 and invasion of MDA-MB-231 cells without effecting cell viability. Among the 20 drugs,
131 Hexachlorophene and Nitazoxanide were removed since the primary targets of the drugs,
132 D-lactate dehydrogenase and pyruvate ferredoxin oxidoreductase are not expressed in
133 mammalian cells. With the exception of Ipriflavone, whose target is still unclear, the
134 known primary targets of the remaining 17 drugs are reported to be expressed by
135 mammalian cells (Figure 2A and Table 1).
136 We confirmed if highly metastatic human cancer cell lines expressed the genes
137 that code for these targets using Western blotting analyses. Among the genes, serotonin
138 receptor 2C (HTR2C), which is a primary target of Pizotifen, was highly expressed in
139 only metastatic cell lines (Figure 2B). Pizotifen suppressed cell motility and invasion of
140 several highly metastatic human cancer cell lines in a dose-dependent manner (Figure
141 2C). Similarly, Dopamine receptor D2 (DRD2), which is a primary target of S(-)
142 Eticlopride hydrochloride, was highly expressed in only metastatic cell lines, and the drug
143 suppressed cell motility and invasion of these cells in a dose-dependent manner (Figure
144 S2).
145 These results indicate that a number of the epiboly-interrupting drugs also have
146 suppressor effects on cell motility and invasion of highly metastatic human cancer cells.
147
148 **Pizotifen suppressed metastatic dissemination of human cancer cells in a zebrafish**
149 **xenotransplantation model.**
150 While a number of the epiboly-interrupting drugs suppressed cell motility and invasion of
151 human cell lines *in vitro,* it was still unclear whether the drugs could suppress metastatic
152 dissemination of cancer cells in vivo. Therefore, we examined whether the identified
153 drugs could suppress metastatic dissemination of these human cancer cells in a zebrafish
154 xenotransplantation model. Pizotifen was selected to test since HTR2C was overexpressed
155 only in highly metastatic cell lines supporting the hypothesis that it could be a novel target

156 for blocking metastatic dissemination of cancer cells (Figure 2B). Red fluorescent
157 protein-labelled MDA-MB-231 (231R) cells were injected into the duct of Cuvier of *Tg*
158 *(kdrl:eGFP)* zebrafish at 2 dpf and then maintained in the presence of either vehicle or
159 Pizotifen. Twenty-four hours post-injection, the numbers of fish showing metastatic
160 dissemination of 231R cells were measured via fluorescence microscopy. In this model,
161 the dissemination patterns were generally divided into three categories: (i) head
162 dissemination, in which disseminated 231R cells exist in the vessel of the head part; (ii)
163 trunk dissemination, in which the cells were observed in the vessel dilating from the trunk
164 to the tail; (iii) end-tail dissemination, in which the cells were observed in the vessel of
165 the end-tail part (16).

166 Three independent experiments revealed that the frequencies of fish in the drug-
167 treated group showing head, trunk, or end-tail dissemination, significantly decreased to
168 55.3±7.5%, 28.5±5.0% or 43.5±19.1% when compared with those in the vehicle-treated
169 group; 95.8±5.8%, 47.1±7.7% or 82.6±12.7%. Conversely, the frequency of the fish in the
170 drug-treated group not showing any dissemination, significantly increased to 45.4±0.5%
171 when compared with those in the vehicle-treated group; 2.0±2.9% (Figure 2D).

172 Similar effects were observed in another xenograft experiments using an RFP-
173 labelled human pancreatic cancer cell line, MIA-PaCa-2 (MP2R). In the drug treated
174 group, the frequencies of the fish showing head, trunk or end-tail dissemination,
175 significantly decreased to 15.3±6.7%, 6.2±1.3%, or 41.1±1.5%; conversely, the frequency
176 of the fish not showing any dissemination significantly increased to 46.3±8.9% when
177 compared with those in the vehicle-treated group; 74.5±11.1%, 18.9±14.9%, 77.0±9.0%,
178 or 17.2±0.7% (Figure S3).

179 To eliminate the possibility that the metastasis suppressing effects of Pizotifen
180 might result from off-target effects of the drug, we conducted validation experiments to
181 determine whether knockdown of HTR2C would show the same effects. Sub-clones of
182 231R cells that expressed shRNA targeting either LacZ or HTR2C were injected into the

183 fish at 2 dpf and the fish were maintained in the absence of drug. In the fish that were
184 inoculated with shHTR2C 231R cells, the frequencies of the fish showing head, trunk,
185 and end-tail dissemination, significantly decreased to 6.7±4.9%, 6.7±0.7%, or
186 20.0±16.5%; conversely, the frequency of the fish not showing any dissemination,
187 significantly increased to 80.0±4.4% when compared with those that were inoculated with
188 shLacZ 231R cells; 80.0±27.1%, 20.0±4.5%, 90.0± 7.7%, or 0% (Figure 2E).
189 These results indicate that pharmacological and genetic inhibition of HTR2C
190 suppressed metastatic dissemination of human cancer cells in vivo.
191
192 **Pizotifen suppressed metastasis progression of a mouse model of metastasis.**
193 We examined the metastasis-suppressor effect of Pizotifen in a mouse model of
194 metastasis (21). Luciferase-expressing 4T1 murine mammary carcinoma cells were
195 inoculated into the mammary fat pads (MFP) of female BALB/c mice. On day two post
196 inoculation, the mice were randomly assigned to two groups and one group received once
197 daily intraperitoneal injections of 10mg/kg Pizotifen while the other group received a
198 vehicle injection. Bioluminescence imaging and tumor measurement revealed that the
199 sizes of the primary tumors in Pizotifen-treated mice were equal to those in the vehicle-
200 treated mice at the time of resection on day 10 post inoculation. Immunofluorescent
201 staining also demonstrated that the percentage of Ki67 positive cells in the resected
202 primary tumors of Pizotifen-treated mice were the same as those of vehicle-treated mice
203 (Figure 3A-C), additionally, both groups showed less than 1% cleaved caspase 3 positive
204 cells (data not shown). Therefore, no anti-tumor effect of Pizotifen was observed on the
205 primary tumor. After 70 days from inoculation, bioluminescence imaging detected light
206 emitted in the lungs, livers and lymph nodes of vehicle-treated mice but not those of
207 Pizotifen-treated mice (Figure 3C). Vehicle-treated mice formed 5 to 50 metastatic
208 nodules per lung in all 10 mice analyzed; conversely, Pizotifen-treated mice (n=10)
209 formed 0 to 5 nodules per lung in all 10 mice analyzed (Figure 3D). Histological analyses

210 confirmed that metastatic lesions in the lungs were detected in all vehicle-treated mice;
211 conversely, they were detected in only 2 of 10 Pizotifen-treated mice and the rest of the
212 mice showed metastatic colony formations around the bronchiole of the lung. In addition,
213 4 of 10 vehicle-treated mice exhibited metastasis in the liver and the rest showed
214 metastatic colony formation around the portal tract of the liver. In contrast, none of 10
215 Pizotifen-treated mice showed liver metastases and only half of the 10 mice showed
216 metastatic colony formation around the portal tract (Figure 3E). These results indicate that
217 Pizotifen can suppress metastasis progression without affecting primary tumor growth.
218 To eliminate the possibility that the metastasis suppressing effects of Pizotifen
219 might result from off-target effects, we conducted validation experiments to determine
220 whether knockdown of HTR2C would show the same effects. The basic experimental
221 process followed the experimental design described above except that sub-clones of 4T1
222 cells that expressed shRNA targeting either LacZ or HTR2C were injected into the MFP
223 of female BALB/c mice and the mice were maintained without drug. Histological
224 analyses revealed that all of the mice (n=5) that were inoculated with 4T1 cells expressing
225 shRNA targeting LacZ showed metastases in the lungs. The mean number of metastatic
226 lesions in a lung was 26.4±7.8. In contrast, only one of the mice (n=5) were inoculated
227 with 4T1 cells expressing shRNA targeting HTR2C showed metastases in the lungs and
228 the rest of the mice showed metastatic colony formation around the bronchiole of the
229 lung. The mean number of metastatic lesions in the lung significantly decreased to 10% of
230 those of mice that were inoculated with 4T1 cells expressing shRNA targeting LacZ
231 (Figure 3F-H).
232 Taken together, pharmacological and genetic inhibition of HTR2C showed an
233 anti-metastatic effect in the 4T1 model system.
234
235 **HTR2C promoted EMT-mediated metastatic dissemination of human cancer cells**

236 Although pharmacological and genetic inhibition of HTR2C inhibited metastasis
237 progression, a role for HTR2C on metastatic progression has not been reported.
238 Therefore, we examined whether HTR2C could confer metastatic properties on poorly
239 metastatic cells.

240 Firstly, we established a stable sub-clone of MCF7 human breast cancer cells
241 expressing either vector control or HTR2C. Vector control expressing MCF7 cells
242 maintained highly organized cell-cell adhesion and cell polarity; however, HTR2C-
243 expressing MCF7 cells led to loss of cell-cell contact and cell scattering. The cobblestone-
244 like appearance of these cells was replaced by a spindle-like, fibroblastic morphology.
245 Western blotting and immunofluorescence (IF) analyses revealed that HTR2C-expressing
246 MCF7 cells showed loss of E-cadherin and EpCAM, and elevated expressions of N-
247 cadherin, vimentin and an EMT-inducible transcriptional factor Zeb1. Similar effects
248 were validated through another experiment using an immortal keratinocyte cell line,
249 HaCaT cells, in that HTR2C-expressing HaCaT cells also showed loss of cell-cell contact
250 and cell scattering with loss of epithelial markers and gain of mesenchymal markers
251 (Figure 4A-C). Therefore, both the morphological and molecular changes in the HTR2C-
252 expressing MCF7 and HaCaT cells demonstrated that these cells had undergone an EMT.

253 Next, we examined whether HTR2C-driven EMT could promote metastatic
254 dissemination of human cancer cells. Boyden chamber assay revealed that HTR2C
255 expressing MCF7 cells showed an increased cell motility and invasion compared with
256 vector control-expressing MCF7 cells in vitro (Figure 4D). Moreover, we conducted in
257 vivo examination of whether HTR2C expression could promote metastatic dissemination
258 of human cancer cells in a zebrafish xenotransplantation model. Red fluorescence protein-
259 labelled MCF7 cells expressing either vector control or HTR2C were injected into the
260 duct of Cuvier of *Tg* (*kdrl:eGFP*) zebrafish at 2 dpf. Twenty-four hours post injection, the
261 frequencies of the fish showing metastatic dissemination of the inoculated cells were
262 measured using fluorescence microscopy. In the fish that were inoculated with HTR2C

263 expressing MCF7 cells, the frequencies of the fish showing head, trunk, and end-tail
264 dissemination significantly increased to 96.7±4.7%, 68.8±6.4%, or 89.5±3.4%;
265 conversely, the frequency of the fish not showing any dissemination decreased to 0%
266 when compared with those in the fish that were inoculated with vector control expressing
267 MCF7 cells; 33.1±18.5%, 0%, 56.9± 4.4%, or 43% (Figure 4E).
268 These results indicated that HTR2C promoted metastatic dissemination of cancer
269 cells though induction of EMT, and suggest that the screen can easily be converted to a
270 chemical genetic screening platform.
271
272 **Pizotifen induced mesenchymal to epithelial transition through inhibition of Wnt-**
273 **signaling.**
274 Finally, we elucidated the mechanism of action of how Pizotifen suppressed metastasis,
275 especially metastatic dissemination of cancer cells. Our results showed that HTR2C
276 induced EMT and that pharmacological and genetic inhibition of HTR2C suppressed
277 metastatic dissemination of MDA-MB-231 cells that had already transitioned to
278 mesenchymal-like traits via EMT. Therefore, we speculated that blocking HTR2C with
279 Pizotifen might inhibit the molecular mechanisms which follow EMT induction. We
280 firstly investigated the expressions of epithelial and mesenchymal markers in Pizotifen-
281 treated MDA-MB-231 cells since the activation of an EMT program needs to be transient
282 and reversible, and transition from a fully mesenchymal phenotype to a epithelial-
283 mesenchymal hybrid state or a fully epithelial phenotype is associated with malignant
284 phenotypes (22). IF and FACS analyses revealed 20% of Pizotifen-treated MDA-MB-231
285 cells restored E-cadherin expression. Also, western blotting analysis demonstrated that
286 4T1 primary tumors from Pizotifen-treated mice has elevated E-cadherin expression
287 compared with tumors from vehicle-treated mice (Figure 5A-C). However, mesenchymal
288 markers did not change between vehicle and Pizotifen-treated MDA-MB-231 cells (data
289 not shown). We further analyzed E-cadherin positive (E-cad^{+}) cells in Pizotifen-treated

290 MDA-MB-231 cells. The E-cad$^+$ cells showed elevated expressions of epithelial markers
291 KRT14 and KRT19; and decreased expression of mesenchymal makers vimentin, MMP1,
292 MMP3, and S100A4. Recent research reports that an EMT program needs to be transient
293 and reversible and that a mesenchymal phenotype in cancer cells is achieved by
294 constitutive ectopic expression of Zeb1. In accordance with the research, the E-cad$^+$ cells
295 and 4T1 primary tumors from Pizotifen-treated mice had decreased Zeb1 expression
296 compared with vehicle-treated cells and tumors from vehicle-treated mice (Figure 5D). In
297 contrast, HTR2C-expressing MCF7 and HuMEC cells expressed Zeb1 but not vehicle
298 control MCF7 and HuMEC cells (Figure 4C). These results indicate that HTR2C-
299 mediated signaling induced EMT through up-regulation of Zeb1 and blocking HTR2C
300 with Pizotifen induced mesenchymal to epithelial transition through downregulation of
301 Zeb1.

302 We further investigated the mechanism of action of how blocking HTR2C with
303 Pizotifen induced down-regulation of Zeb1. In embryogenesis, serotonin-mediated
304 signaling is required for Wnt-dependent specification of the superficial mesoderm during
305 gastrulation (23). In cancer cells, overexpression of HTR1D is associated with Wnt-
306 signaling which enables induction of EMT (24, 25). This evidence led to a hypothesis that
307 HTR2C-mediated signaling might turn on transcriptional activity of β-catenin and that
308 might induce up-regulation of EMT-TFs. IF analyses revealed β-catenin was accumulated
309 in the nucleus of HTR2C-expressing MCF7 cells but it was located in the cytoplasm of
310 vector control-expressing cells (Figure 5E). Nuclear accumulation of β-catenin in
311 HTR2C-expressing MCF7 cells was confirmed by western blot (Figure 5F). In contrast,
312 Pizotifen-treated MDA-MB-231 cells showed β-catenin located in the cytoplasm of the
313 cells. Vehicle-treated cells showed β-catenin accumulated in the nucleus of the cells.
314 (Figure 5G), and western blotting analysis confirmed that it was located in the cytoplasm
315 of Pizotifen-treated MDA-MB-231 cells (Figure 5H). Furthermore,
316 immunohistochemistry and western blotting analyses showed that β-catenin accumulated

317 in the nucleus, and phospho-GSKβ and Zeb1 expression were decreased in 4T1 primary
318 tumors from Pizotifen-treated mice compared with vehicle-treated mice (Figure 5C).
319 These results indicated that HTR2C would regulate transcriptional activity of β-catenin
320 and Pizotifen could inhibit it.
321 Taken together, we conclude that blocking HTR2C with Pizotifen restored
322 epithelial properties to metastatic cells (MDA-MB-231 and 4T1 cells) through a decrease
323 of transcriptional activity of β-catenin and that suppressed metastatic progression of the
324 cells.
325

326 **Figures and figure legends**

327 **Figure 1**

328

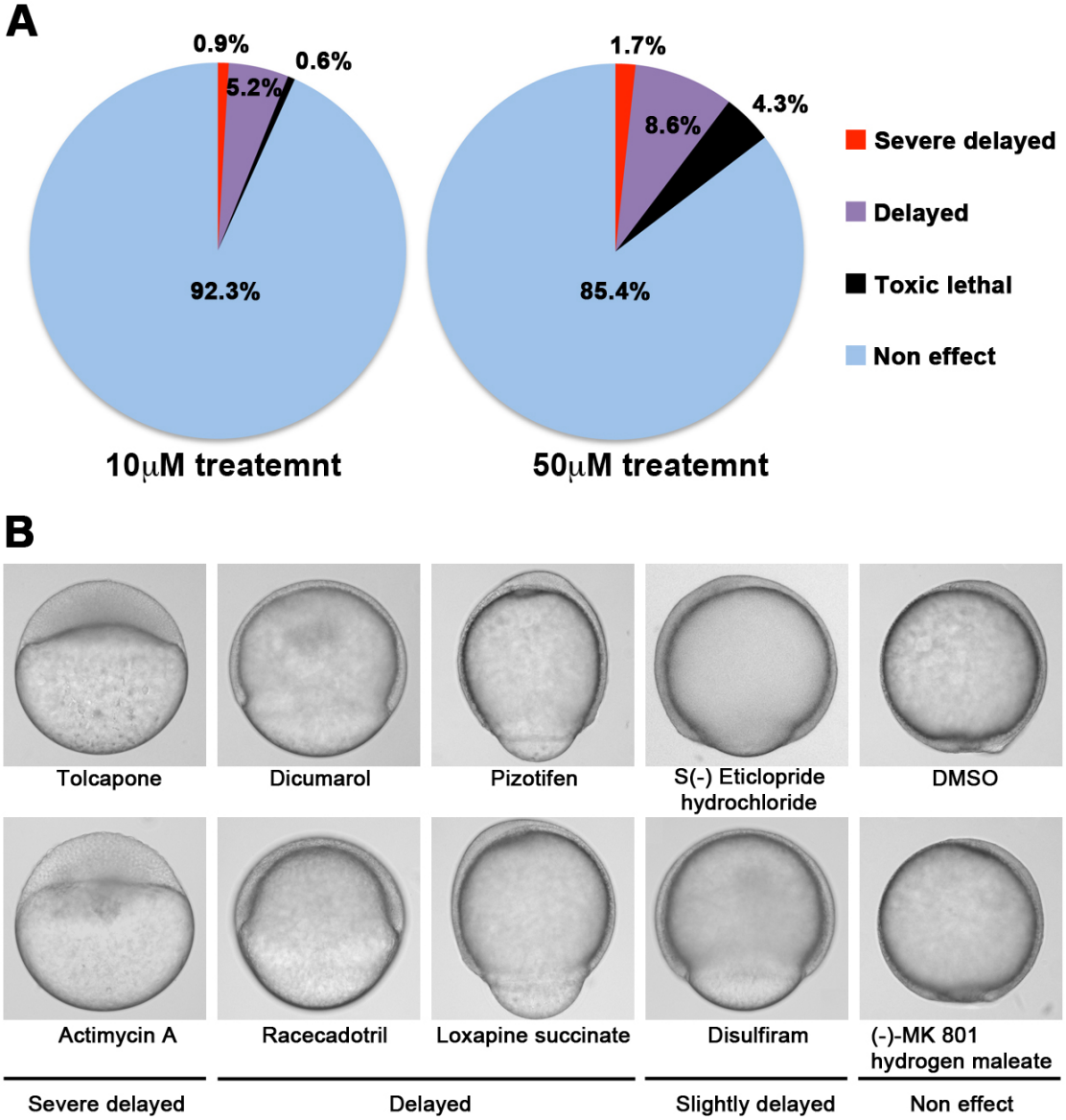

329

330

331 **Figure 1. A chemical screen for identification of epiboly-interrupting drugs.**

332 (A) Cumulative results of the chemical screen in which each drug was used at either

333 10μM (left) or 50μM (right) concentrations. 1,280 FDA, EMA or other agencies-

334 approved drugs were subjected to this screening. Positive "hit" drugs were those that

335 interrupted epiboly progression. (B) Representative samples of the embryos that were

336 treated with indicated drugs.

337 **Figure 2**

338

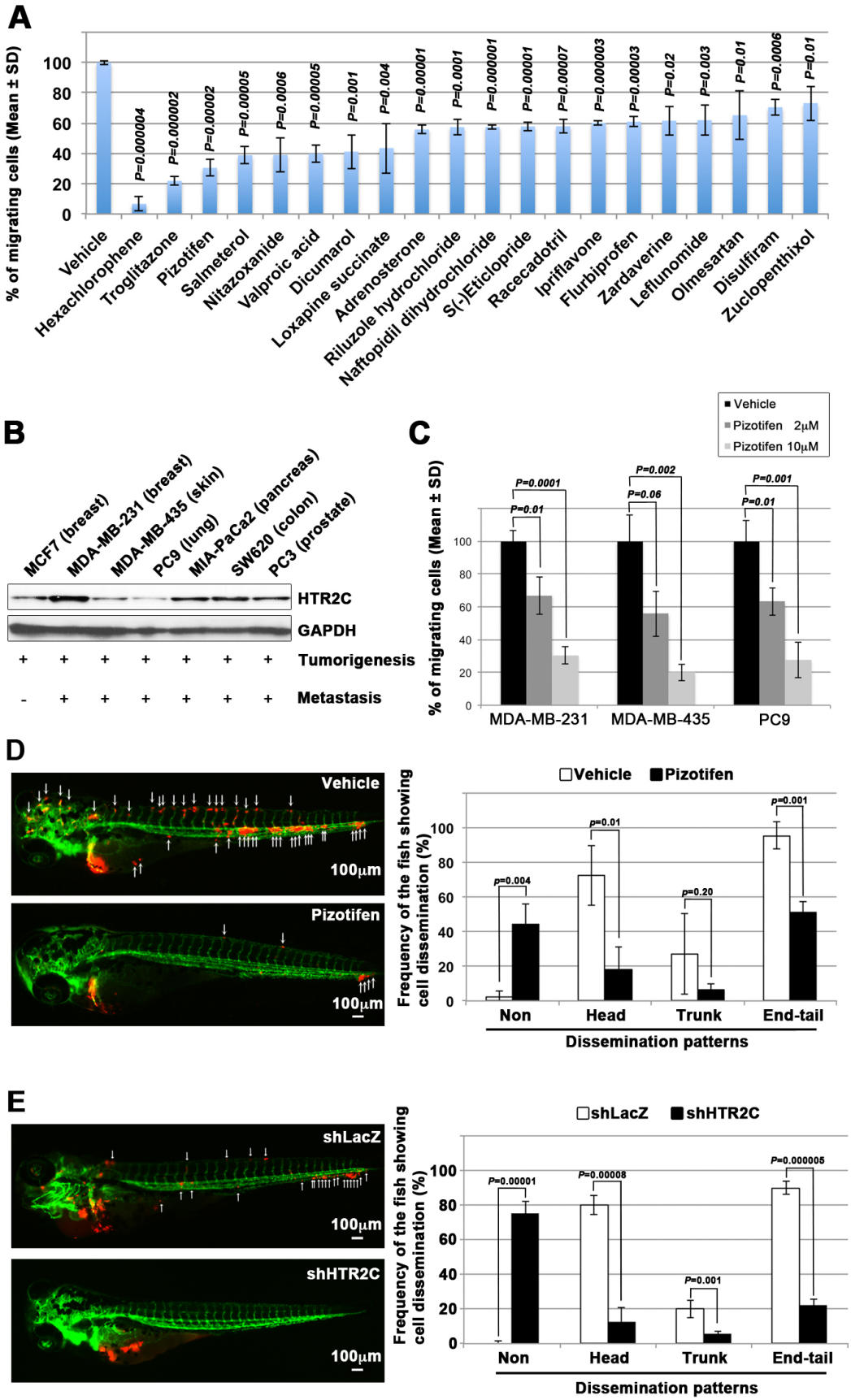

339

340 **Figure 2. Pizotifen, one of epiboly-interrupting drugs suppressed metastatic**

341 **dissemination of human cancer cells lines in vivo and vitro.**

342 (A) Effect of the epiboly-interrupting drugs on cell motility and invasion of MBA-MB-
343 231 cells. MBA-MB-231 cells were treated with vehicle or each of the epiboly-
344 interrupting drugs and then subjected to Boyden chamber assays. Fetal bovine serum
345 (1%v/v) was used as the chemoattractant in both assays. Each experiment was performed
346 at least twice. (B) Western blot analysis of HTR2C levels (top) in a non-metastatic human
347 cancer cell line, MCF7 (breast) and highly metastatic human cancer cell lines, MDA-MB-
348 231 (breast), MDA-MB-435 (melanoma), PC9 (lung), MIA-PaCa2 (pancreas), PC3
349 (prostate) and SW620 (colon); GAPDH loading control is shown (bottom). (C) Effect of
350 pizotifen on cell motility and invasion of MBA-MB-231, MDA-MB-435 and PC9 cells.
351 Either vehicle or pizotifen treated the cells were subjected to Boyden chamber assays.
352 Fetal bovine serum (1%v/v) was used as the chemoattractant in both assays. Each
353 experiment was performed at least twice. (D) and (E) Representative images of
354 dissemination of 231R, shLacZ 231R or shHTR2C 231R cells in zebrafish
355 xenotransplantation model. The fish larvae that were inoculated with 231R cells, were
356 treated with either vehicle (top left) or the drug (lower left) (D). The fish larvae that were
357 inoculated with either shLacZ 231R or shHTR2C 231R cells (lower left) (E). White
358 arrows head indicate disseminated 231R cells. The images were shown in 4x
359 magnification. Scale bar, 100μm. The mean frequencies of the fish showing head, trunk,
360 or end-tail dissemination were counted (graph on right). Each value is indicated as the
361 mean ± SEM of two independent experiments. Statistical analysis was determined by
362 Student's t test. See also Figure S2 and S3.
363

364 **Figure 3**

365

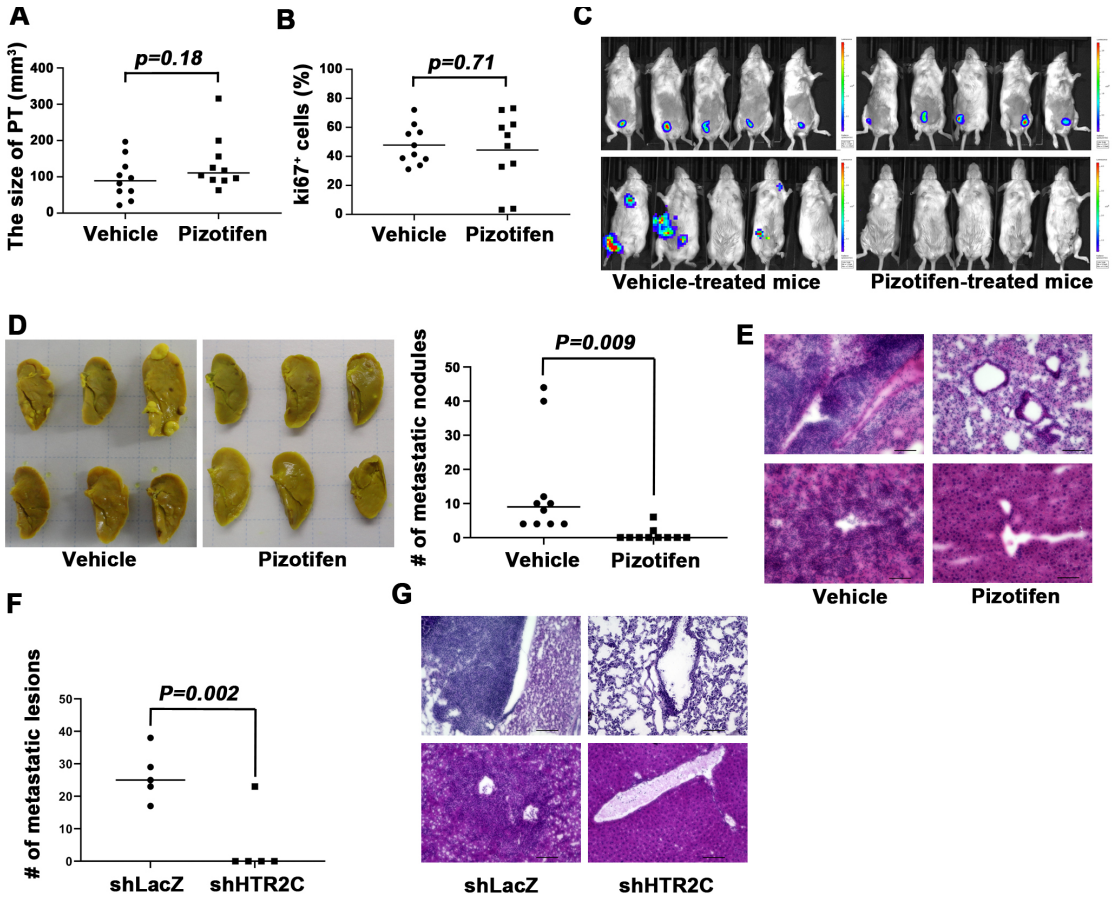

366

367

368 **Figure 3. Pizotifen suppressed metastatic progression in a mouse model of**

369 **metastasis.**

370 (A) Mean volumes (n=10 per group) of 4T1 primary tumors formed in the mammary fat

371 pad of either vehicle or Pizotifen-treated mice at day 10 post injection. (B) Ki67

372 expression level in 4T1 primary tumors formed in the mammary fat pad of either vehicle

373 or Pizotifen-treated mice at day 10 post injection. The mean expression levels of Ki67

374 (n=10 mice per group) were determined and were calculated as the mean ration of Ki67

375 positive cells to DAPI area. (C) Representative images of primary tumors on day 10 post

376 injection (top panels) and metastatic burden on day 70 post injection (bottom panels)

377 taken using an IVIS Imaging System. (D) Representative images of the lungs from either

378 vehicle (top) or Pizotifen-treated mice (bottom) at 70 days past tumor inoculation.

379 Number of metastatic nodules in the lung of either vehicle or Pizotifen-treated mice
380 (right). (E) Representative H&E staining of the lung (top) and liver (bottom) from either
381 vehicle or Pizotifen-treated mice. (F) The mean number of metastatic lesions in step
382 sections of the lungs from the mice that were inoculated with 4T1-12B cells expressing
383 shRNA targeting for either LacZ or HTR2C. (G) Representative H&E staining of the lung
384 and liver from the mice that were inoculated with 4T1-12B cells expressing shRNA
385 targeting for either LacZ or HTR2C. Each value is indicated as the mean ± SEM.
386 Statistical analysis was determined by Student's *t* test.
387

388 **Figure 4**

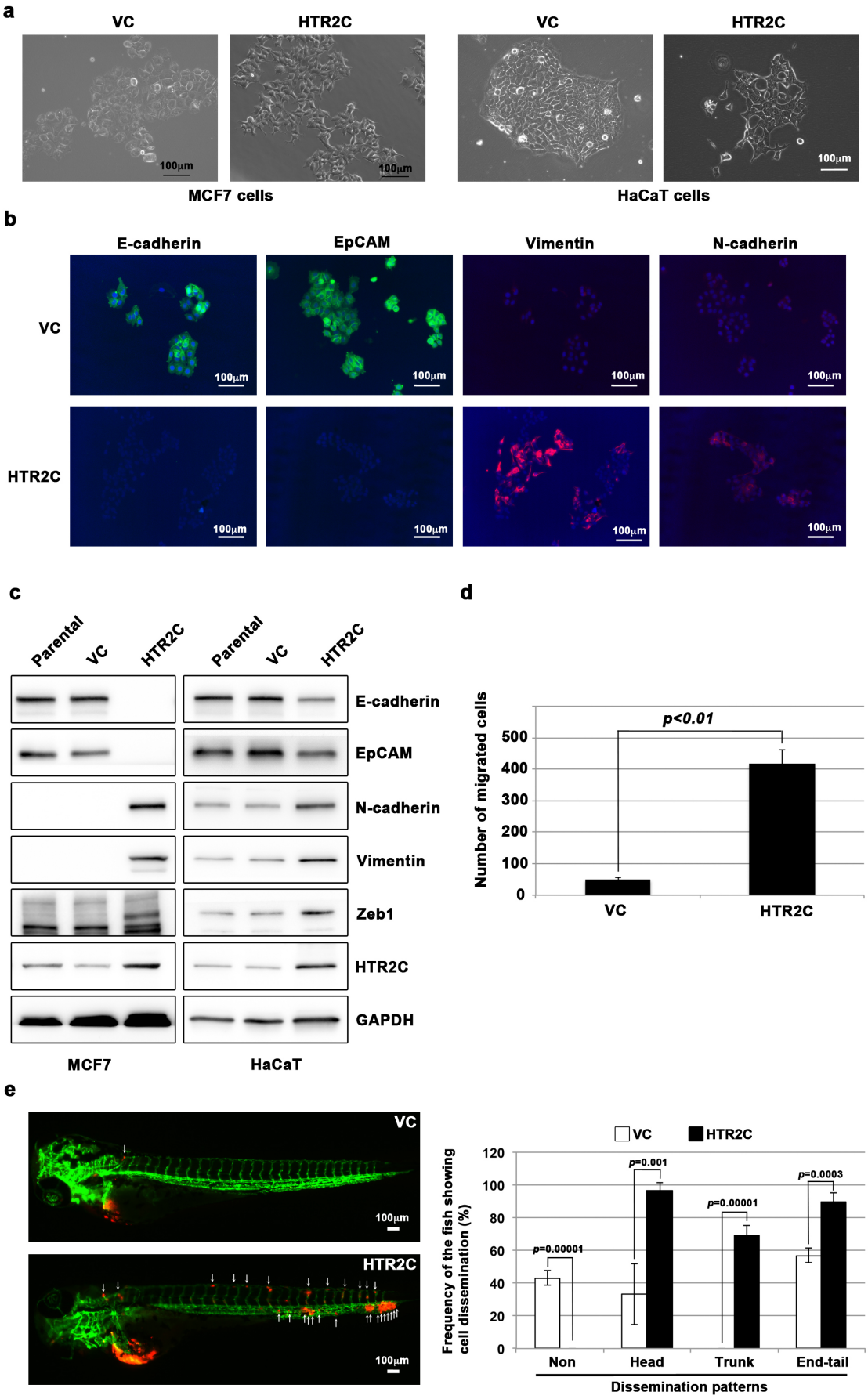

389

390 **Figure 4. HTR2C induced EMT-mediated metastatic dissemination of human cancer**
391 **cells.**
392 (A) The morphologies of the MCF7 and HaCaT cells expressing either the control vector
393 or HTR2C were revealed by phase contrast microscopy. (B) Immunofluorescence staining
394 of E-cadherin, EpCAM, Vimentin, and N-cadherin expressions in the MCF7 cells from
395 Figure 4A. (C) Expression of E-cadherin, EpCAM, Vimentin, N-cadherin, and HTR2C
396 was examined by western-blotting in the MCF7 and HaCaT cells; GAPDH loading
397 control is shown (bottom). (D) Effect of HTR2C on cell motility and invasion of MCF7
398 cells. MCF7 cells were subjected to Boyden chamber assays. Fetal bovine serum (1%v/v)
399 was used as the chemoattractant in both assays. Each experiment was performed at least
400 twice. (E) Representative images of dissemination patterns of MCF7 cells expressing
401 either the control vector (top left) or HTR2C (lower left) in a zebrafish
402 xenotransplantation model. White arrows head indicate disseminated MCF7 cells. The
403 mean frequencies of the fish showing head, trunk, or end-tail dissemination tabulated
404 (right). Each value is indicated as the mean ± SEM of two independent experiments.
405 Statistical analysis was determined by Student's *t* test.
406

407 **Figure 5**

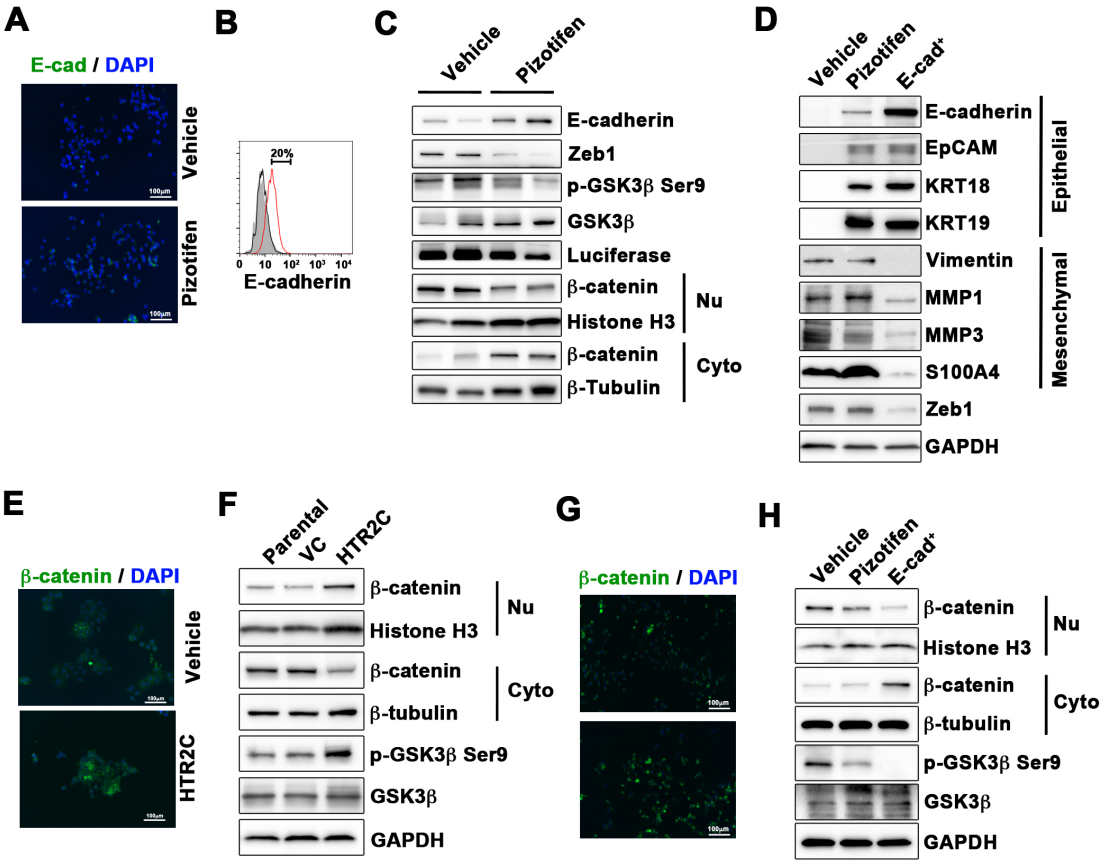

408

409 **Figure 5. Pizotifen restored mesenchymal-like traits of MDA-MB-231 cells into**

410 **epithelial traits through blocking nuclear accumulation of β-catenin.**

411 (A) IF staining of E-cadherin in either vehicle or Pizotifen-treated MDA-MB-231 cells.

412 (B) Surface expression of E-cadherin in either vehicle (black) or Pizotifen (red)-treated

413 MDA-MB-231 cells by FACS analysis. Non-stained controls are shown in gray. (C)

414 Protein expressions levels of E-cadherin, Zeb1, and β-catenin in the cytoplasm and

415 nucleus of 4T1 primary tumors from either vehicle or Pizotifen-treated mice are shown;

416 Luciferase, Histone H3, and β-tubulin are used as loading control for whole cell, nuclear

417 or cytoplasmic lysate, respectively. (D) Protein expression levels of epithelial and

418 mesenchymal markers and Zeb1 in either vehicle or Pizotifen-treated MDA-MB-231 cells

419 or E-cadherin positive (E-cad^{+}) cells in Pizotifen-treated MDA-MB-231 cells are shown.

420 (E) Immunofluorescence staining of β-catenin in the MCF7 cells expressing either vector

421 control or HTR2C. (F) Expressions of β-catenin in the cytoplasm and nucleus of MCF7

422 cells. (G) IF staining of β-catenin in either vehicle or Pizotifen-treated MDA-MB-231

423 cells. (H) Expressions of β-catenin in the cytoplasm and nucleus of MDA-MB-231 cells

424 and the E-cad^{+} cells.

425

426 **Table 1. Primary targets of the identified drugs**
427

The identified drugs	Primary targets of the identified drugs
Hexachlorophene	D-lactate dehydrogenase (D-LDH), not expressed in mammalian cells
Troglitazone	Agonist for Peroxisome proliferator-activated receptor α and γ (PPARα and γ)
Pizotifen malate	5-hydroxytryptamine receptor 2C (HTR2C)
Salmeterol	Adrenergic receptor beta 2 (ADRB2)
Nitazoxanide	Pyruvate ferredoxin oxidoreductase (PFOR), not expressed in mammalian cells
Valproic acid	Histone deacetylases (HDACs)
Dicumarol	NAD(P)H dehydrogenase quinone 1 (NQO1)
Loxapine succinate	Dopamine receptor D2 and D4 (DRD2 and DRD4)
Adrenosterone	Hydroxysteroid (11-beta) dehydrogenase 1 (HSD11β1)
Riluzole hydrochloride	Glutamate R and Voltage-dependent Na+ channel
Naftopidil dihydrochloride	5-hydroxytryptamine receptor 1A (HTR1A) and α1-adrenergic receptor (AR)
S(-)Eticlopride hydrochloride	Dopamine receptor D2 (DRD2)
Racecadotril	Membrane metallo-endopeptidase (MME)
Ipriflavone	Unknow
Flurbiprofen	Cyclooxygenase 1 and 2 (Cox1 and 2)
Zardaverine	Phosphodiesterase III/IV (PDE3/4)
Leflunomide	Dihydroorotate dehydrogenase (DHODH)
Olmesartan	Angiotensin II receptor alpha
Disulfiram	Aldehyde dehydrogenase (ALDH) Dopamine β-hydroxylase (DBH)
Zuclopenthixol dihydrochloride	Dopamine receptors D1 and D2 (DRD1 and 2)

428
429 **Discussion**

430 Reducing or eliminating mortality associated with metastatic disease is a key goal of
431 medical oncology, but few models exist that allow for rapid, effective screening of novel
432 compounds that target the metastatic dissemination of cancer cells. Based on accumulated

433 evidence that at least fifty genes play an essential role in governing both metastasis and
434 gastrulation progression (Table 1S), we hypothesized that small molecule inhibitors that
435 interrupt gastrulation of zebrafish embryos might suppress metastatic progression of
436 human cancer cells. We created a unique screening concept utilizing gastrulation of
437 zebrafish embryos to test the hypothesis. Our results clearly confirmed our hypothesis:
438 25.6% (20/76 drugs) of epiboly-interrupting drugs could also suppress cell motility and
439 invasion of highly metastatic human cell lines in vitro. In particular, Pizotifen which is an
440 antagonist for serotonin receptor 2C and one of the epiboly-interrupting drugs, could
441 suppress metastasis in a mouse model (Figure 3A-E). Thus, this screen could offer a novel
442 platform for discovery of anti-metastasis drugs.
443 There are at least two advantages to the screen described herein. One is that the
444 screen can easily be converted to a chemical genetic screening platform. Indeed, we have
445 provided the first evidence that HTR2C, which is a primary target of Pizotifen, induced
446 EMT and promoted metastatic dissemination of cancer cells (Figure 4A-E). In this
447 research, 1,280 FDA approval drugs were screened, this is less than a few percent of all of
448 druggable targets (approximately 100 targets) in the human proteome in the body. If
449 chemical genetic screening using specific inhibitor libraries were conducted, more genes
450 that contribute to metastasis and gastrulation could be identified. The second advantage is
451 that the screen enables one researcher to test 100 drugs in 5 hours with using optical
452 microscopy, drugs, and zebrafish embryos. That indicates this screen is not only highly
453 efficient, low-cost, and low-labor but also enables researchers who do not have high
454 throughput screening instruments to conduct drug screening for anti-metastasis drugs.
455

456 **Acknowledgments**

457 We sincerely appreciate Dr. Joshua Collins (NIH/NIDCR) and Dr. Diane Palmieri
458 (NIH/NCI) for helping this research. We thank Dr. Herrick (Albany medical collage) for
459 providing pCMV-h5TH2C-VSV with us. This study was funded by grants from National

460 Medical Research Council of Singapore (R-154000547511) and Ministry of Education of
461 Singapore (R-154000A23112) to Z.G.
462

463 **Author Contributions**

464 Design research; J.N. Conducting experiments; J.N. and L.T. Analyzing data: J.N.
465 Writing the paper; J.N. and Z.G. Funding Acquisition; Z.G, S.W. B.C.G., H.M. and
466 Supervision; Z.G.
467

468 **Declaration of Interests**

469 J.N., L.T., B.C.G., S.W., H.M. and G.Z. declare no conflict of interest.
470

471 **Materials and Methods**

472 **Zebrafish embryo screening**

473 Each drug was added to a well of a 24-well plate containing approximately 20 zebrafish
474 embryos per well in either 10 μM or 50 μM final concentration when the embryos reached
475 the sphere stage. Chemical treatment was initiated at 4 hours post-fertilization (hpf) and
476 approximately 20 embryos were treated with two different concentrations for each
477 compound tested. The treatment was ended at 9 hpf when vehicle (DMSO) treated
478 embryos as control reach 80-90% completion of the epiboly stage. The compounds which
479 induced delay (<50% epiboly) in epiboly were selected as hit compounds for in vitro
480 testing using highly metastatic human cancer cell lines. The study protocol was approved
481 by the Institutional Animal Care and Use Committee of the National University of
482 Singapore (protocol number: R16-1068).
483

484 **Reagents**

485 FDA, EMA and other agencies approved chemical libraries was purchased from
486 Prestwick Chemical (Illkirch, France). Pizotifen and S(-) Eticlopride hydrochloride were
487 purchased from Sigma-Aldrich (St. Louis, MO).
488
489 **Cell culture and cell viability assay**
490 MCF7, MDA-MB-231, MDA-MB-435, MIA-PaCa2, PC3, SW620, PC9 and HaCaT cells
491 were obtained from American Type Culture Collection (ATCC, Manassas, VA).
492 HCCLM3 cells were provided by Dr. Tang, Zhong Shan Hospital of Fudan University
493 (Shanghai, China). Luciferase-expressing 4T1 (4T1-12B) cells were provided from Dr.
494 Gary Sahagian (Tufts University, Boston, MA). All culture methods followed the
495 supplier's instruction. Cell viability assay was performed as previously described (16).
496
497 **Plasmid**
498 A DNA fragment coding for HTR2C was amplified by PCR with primers containing
499 restriction enzyme recognition sequences. The HTR2C coding fragment was amplified
500 from hsp70l:mCherry-T2A-CreERT2 plasmid (17).
501
502 **Immunoblotting**
503 Western blotting was performed as described previously (16). Anti-PRMT1, anti-
504 CYP11A1, anti-E-cadherin, anti-EpCAM, anti-Vimentin, anti-N-cadherin, anti-Zeb1,
505 anti-Histone H_3, anti-α-tubulin and anti-GAPDH antibodies were purchased from Cell
506 signaling Technology. Anti-HTR2C and anti-DRD2 antibodies were purchased form
507 Abcam. Anti-phospho-GSK3β (Ser9), anti-GSK3β, Anti-KRT18, anti-KRT19, anti-
508 MMP1, anti-MMP2, anti-S100A4, anti-Luciferase, and anti-β-catenin antibodies were
509 purchased from Santa Cruz.
510
511 **Flow cytometry**

512 Cells were stained with FITC-conjugated E-cadherin antibody (Biolegend, San Diego,
513 CA). Flow cytometry was performed as described (26) and analyzed with FlowJo
514 software (TreeStar, Ashland, OR).
515
516 **shRNA mediated gene knockdown**
517 The short hairpin RNA (shRNA)-expressing lentivirus vectors were
518 constructed using pLVX-shRNA1 vector (Clontech). PRMT1-shRNA_#3–targeting
519 sequence is GTGTTCCAGTATCTCTGATTA; PRMT1-shRNA_#4–targeting sequence
520 is TTGACTCCTACGCACACTTTG. CYP11A1-shRNA_#4–targeting sequence is
521 GCGATTCATTGATGCCATCTA; CYP11A1-shRNA_#4–targeting sequence is
522 GAAATCCAACACCTCAGCGAT. Human HTR2C-shRNA–targeting sequence is
523 TCATGCACCTCTGCGCTATAT. Mouse HTR2C-shRNA–targeting sequence is . LacZ-
524 shRNA– targeting sequence is CTACACAAATCAGCGATT.
525
526 **Immunofluorescence**
527 Immunofluorescence microscopy assay was performed by previously described (16). Goat
528 anti-mouse and goat anti-rabbit immunoglobulin G (IgG) antibodies conjugated to Alexa
529 Fluor 488 (Life Technologies) and diluted at 1:100 were used. Nuclei were visualized by
530 the addition of 2μg/ml of 4', 6-diamidino-2-phenylindole (DAPI) and photographed at
531 100x magnification by a fluorescent microscope BZ-X700 (KEYENCE, Japan).
532
533 **Boyden chamber cell motility and invasion assay**
534 These assays were performed by previously described (16). In Boyden chamber assay,
535 either $3x10^5$ MDA-MB-231, $1x10^6$ MDA-MB-435, or $5x10^5$ PC9 cells were applied to
536 each well in the upper chamber.
537
538 **Zebrafish xenotransplantation model**

539 *Tg(kdrl:eGFP)* zebrafish was provided by Dr. Stainier (Max Planck Institute for Heart and
540 Lung Research). Embryos that were derived from the line were maintained in E3 medium
541 containing 200μM 1-phenyl-2-thiourea (PTU). Approximately 100-400 Red fluorescence
542 protein (RFP)-labelled MBA-MB-231 or MIA-Paca2 cells were injected into the duct of
543 Cuvier of the zebrafish at 2dpf.
544
545 **Spontaneous metastasis mouse model**
546 4T1-12B cells ($2x10^4$) were injected into the #4 mammary fat pad while the mice were
547 anesthetized. To monitor tumor growth and metastases, mice were imaged biweekly by
548 IVIS Imaging System (ParkinElmer). The primary tumor was resected 10 days after
549 inoculation. The study protocol (protocol number: BRC IACUC #110612) was approved
550 by A*STAR (Agency for Science, Technology and Research, Singapore).
551
552 **Histological Analysis**
553 All OCT embedded primary tumors, lungs, and livers of mice from the spontaneous
554 metastasis 4T1 model were sectioned on a cryostat. Eight micron sections were taken at
555 five hundred micron intervals through the entirety of the livers and lungs. Sections were
556 subsequently stained with hematoxylin and eosin. Metastatic lesions were counted under a
557 microscope in each section for both lungs and livers.
558
559 **Statistics**
560 Data were analyzed by Student's t test; $p < 0.05$ was considered significant.
561
562 **References**

563 1. Chambers AF, Groom AC, & MacDonald IC (2002) Dissemination and growth
564 of cancer cells in metastatic sites. *Nature reviews. Cancer* 2(8):563-572.
565 2. Steeg PS (2003) Metastasis suppressors alter the signal transduction of
566 cancer cells. *Nature reviews. Cancer* 3(1):55-63.
567 3. Fidler IJ (2003) The pathogenesis of cancer metastasis: the 'seed and soil'
568 hypothesis revisited. *Nature reviews. Cancer* 3(6):453-458.

4. Cavallaro U & Christofori G (2004) Cell adhesion and signalling by cadherins and Ig-CAMs in cancer. *Nature reviews. Cancer* 4(2):118-132.
5. Ellenbroek SI, Iden S, & Collard JG (2012) Cell polarity proteins and cancer. *Semin Cancer Biol* 22(3):208-215.
6. Tsai JH & Yang J (2013) Epithelial-mesenchymal plasticity in carcinoma metastasis. *Genes & development* 27(20):2192-2206.
7. Solnica-Krezel L (2005) Conserved patterns of cell movements during vertebrate gastrulation. *Curr Biol* 15(6):R213-228.
8. Latimer A & Jessen JR (2010) Extracellular matrix assembly and organization during zebrafish gastrulation. *Matrix Biol* 29(2):89-96.
9. Solnica-Krezel L (2006) Gastrulation in zebrafish -- all just about adhesion? *Curr Opin Genet Dev* 16(4):433-441.
10. Tsai YJ*, et al.* (2011) The predominant protein arginine methyltransferase PRMT1 is critical for zebrafish convergence and extension during gastrulation. *FEBS J* 278(6):905-917.
11. Hsu HJ, Liang MR, Chen CT, & Chung BC (2006) Pregnenolone stabilizes microtubules and promotes zebrafish embryonic cell movement. *Nature* 439(7075):480-483.
12. Weinbach EC & Garbus J (1969) Mechanism of Action of Reagents that uncouple Oxidative Phosphorylation. *Nature* 221:1016.
13. Sack U*, et al.* (2011) Novel effect of antihelminthic Niclosamide on S100A4-mediated metastatic progression in colon cancer. *Journal of the National Cancer Institute* 103(13):1018-1036.
14. Huang EW*, et al.* (2012) Vinpocetine inhibits breast cancer cells growth in vitro and in vivo. *Apoptosis : an international journal on programmed cell death* 17(10):1120-1130.
15. Szilágyi G*, et al.* (2005) Effects of vinpocetine on the redistribution of cerebral blood flow and glucose metabolism in chronic ischemic stroke patients: a PET study. *Journal of the Neurological Sciences* 229-230:275-284.
16. Nakayama J, Lu J, Makinoshima H, & Gong Z (2020) A Novel Zebrafish Model of Metastasis Identifies the HSD11β1 Inhibitor Adrenosterone as a Suppressor of Epithelial-Mesenchymal Transition and Metastatic Dissemination. *Mol Cancer Res* 18(3):477-487.
17. Kolosionek E*, et al.* (2009) Expression and activity of phosphodiesterase isoforms during epithelial mesenchymal transition: the role of phosphodiesterase 4. *Mol Biol Cell* 20(22):4751-4765.
18. Sasaki T*, et al.* (2014) Serum CD10 is associated with liver metastasis in colorectal cancer. *J Surg Res.* 192(2):390-394.
19. Liu P*, et al.* (2013) Disulfiram targets cancer stem-like cells and reverses resistance and cross-resistance in acquired paclitaxel-resistant triple-negative breast cancer cells. *British journal of cancer* 109(7):1876-1885.
20. Gunnarsson L, Jauhiainen A, Kristiansson E, Nerman O, & Larsson DGJ (2008) Evolutionary conservation of human drug targets in organisms used for environmental risk assessments. *Environmental Science & Technology* 42(15):5807-5813.
21. Tao K, Fang M, Alroy J, & Sahagian GG (2008) Imagable 4T1 model for the study of late stage breast cancer. *BMC cancer* 8:228.
22. Kröger C, Afeyan, A.; Mraz, J.; Eaton, EN.; Reinhardt, F.; Khodor, YL.; Thiru, P.; Bierie B.; Ye, X.; Burge, CB.; Weinberg RA (2019) Acquisition of a hybrid E/M state is essential for tumorigenicity of basal breast cancer cells. *Proceedings of the National Academy of Sciences of the United States of America* 116(15):7353-7362.

621 23. Beyer TD, M.; Thumberger, T.; Vick, P.; Tisler, M.; Schneider, I.; Bogusch, S.;
622 Andre, P.; Ulmer, B.; Walentek, P.; Niesler, B.; Blum, M.; Schweickert, A.
623 (2012) Serotonin signaling is required for Wnt-dependent GRP specification
624 and leftward flow in Xenopus. *Curr Biol* 22(1):33-39.
625 24. Sui HX, H.; Ji, Q.; Liu, X.; Zhou, L.; Song, H.; Zhou, X.; Xu, Y.; Chen, Z.; Cai, J.; Ji, G.;
626 Li, Q. (2015) 5-hydroxytryptamine receptor (5-HT1DR) promotes colorectal
627 cancer metastasis by regulating Axin1/β-catenin/MMP-7 signaling pathway.
628 *Oncotarget* 6(28):25975-25987.
629 25. Zhan TR, N.; Boutros, M. (2017) Wnt signaling in cancer. *Oncogene*
630 36(11):1461–1473.
631 26. Nakayama J*, et al.* (2009) BLNK suppresses pre-B-cell leukemogenesis
632 through inhibition of JAK3. *Blood* 113(7):1483-1492.
633

634

635 **Supplemental Information**

636

637 **Figure S1.**

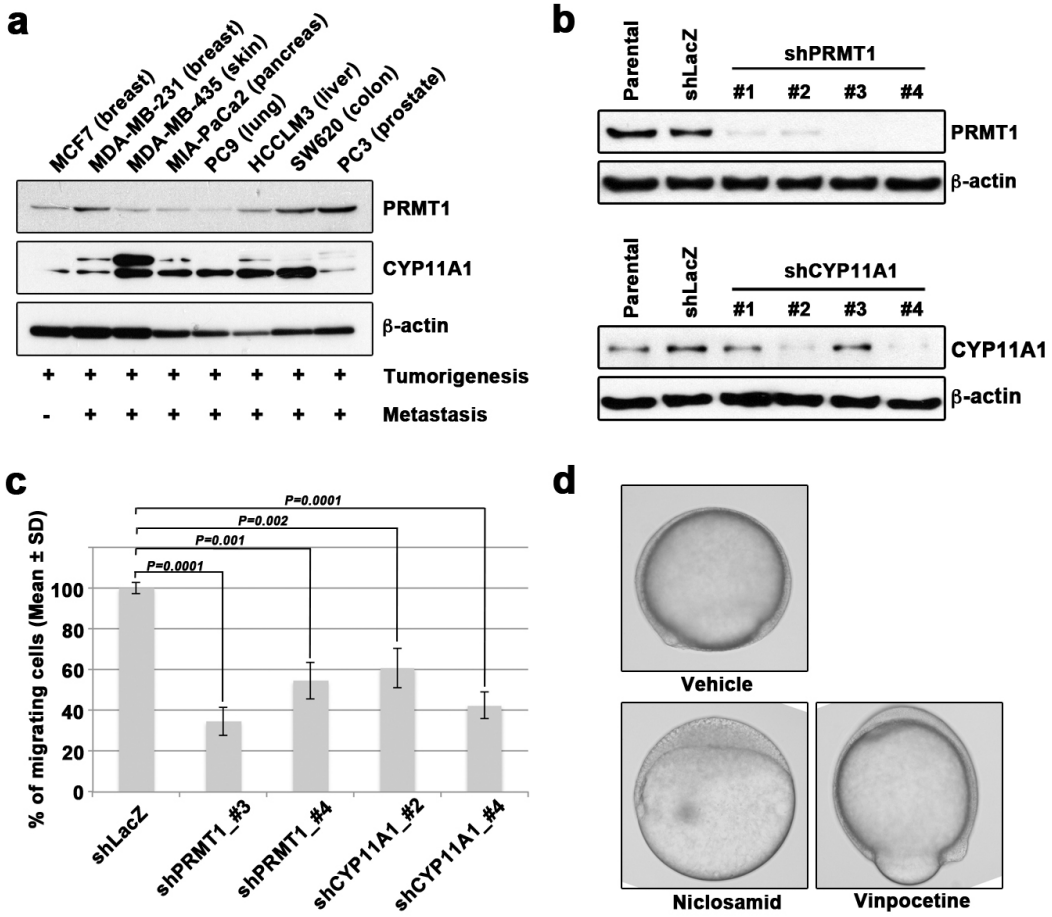

638

639

640 **Figure S1. Molecular mechanisms of epiboly in zebrafish overlap with those in**

641 **cancer metastasis.**

642 (A) Western blot analysis of PRMT1 (upper) and CYP11A1 (middle) protein levels in

643 non-metastatic human cancer cell line (MCF7) and highly metastatic human cancer cell

644 lines (MDA-MB-231, MDA-MB-435, MIA-PaCa2, PC9, HCCLM3, PC3 and SW620); β-

645 actin loading control is shown (bottom). (B) Knockdown of PRMT1 or CYP11A1 in

646 MDA-MB-231 cells. MBA-MB-231 cells were transfected with a control shRNA

647 targeting LacZ, and one of four independent shRNAs targeting PRMT1 (clone #1 to #4)

648 or one of two independent shRNAs targeting CYP11A1 (clone #1 to #4). Reduced

649 PRMT1 and CYP11A1 expression, determined by western blot, in sub-cell lines of MDA-

650 MB-231 cells expressing PRMT1 shRNA (clone #3 and #4 or CYP11A1 (clone #2 and

651 #4), compared with controls (parental cell line MDA-MB-231 and control shRNA cells);

652 β-actin levels shown as a loading control. (C) Effect of shRNAs targeting either PRMT1
653 or CYP11A1 on cell motility and invasion of MBA-MB-231 cells. Parental MDA-MB-
654 231 cells and four sub-cell lines of MDA-MB-231 cells that were transfected with either
655 shRNA targeting either LacZ, two independent shRNAs targeting PRMT1 (clone #3 and
656 #4) or two independent shRNAs targeting CYP11A1 (clone #2 and #4), were subjected to
657 Boyden chamber assays. (D) Zebrafish embryos treated with either vehicle (DMSO),
658 10μM Niclosamide, or 50μM vinpocetine. Approximately 20 embryos were treated with
659 either DMSO as a vehicle control, niclosamide, or vinpocetine. The treatment was started
660 at 4 hpf when all of embryos reached sphere stage and ended at 9 hpf when control
661 embryos reached 80-90% epiboly stage. Each experiment was performed at least twice.
662 Statistical analysis was determined by Student's *t* test.
663

664 **Figure S2.**

665

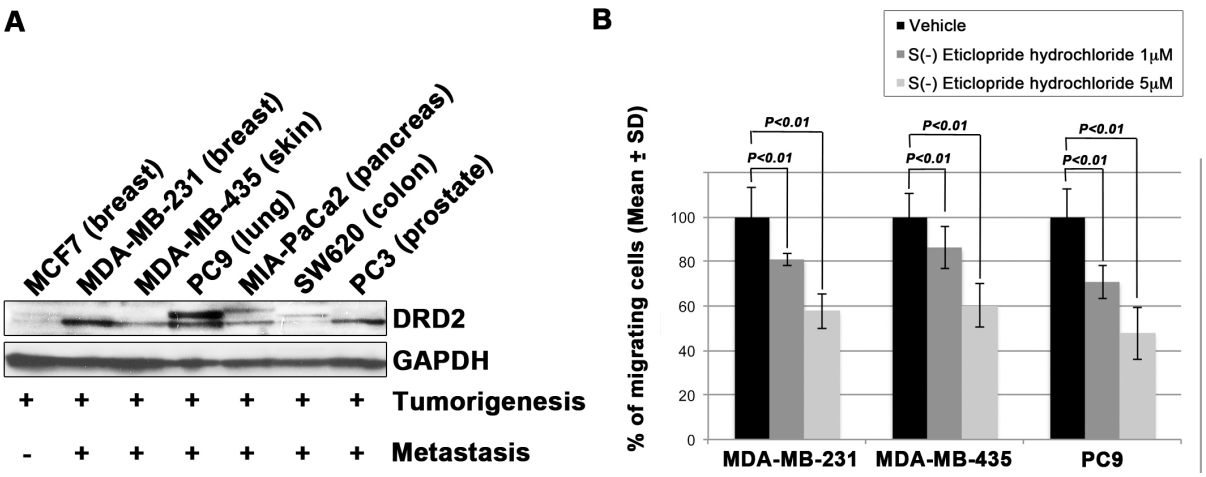

666

667

668 **Figure S2. S (-) Eticlopride hydrochloride suppressed cell motility and invasion of**

669 **human cancer cells.**

670 (A) Western blot analysis of DRD2 levels in non-metastatic human cancer cell line,

671 MCF7 (breast) and highly metastatic human cancer cell lines, MDA-MB-231 (breast),

672 MDA-MB-435 (melanoma), MIA-PaCa2 (pancreas), PC3 (prostate) and SW620 (colon);

673 GAPDH loading control is shown (bottom). (B) Effect of S (-) Eticlopride hydrochloride

674 on cell motility and invasion of MBA-MB-231, MDA-MB-435, and PC9 cells. Either

675 vehicle or pizotifen treated cells were subjected to Boyden chamber assays. Fetal bovine

676 serum (1%v/v) was used as the chemoattractant in both assays. Each experiment was

677 performed at least twice. Statistical analysis was determined by Student's *t* test.

678

679 **Figure S3.**

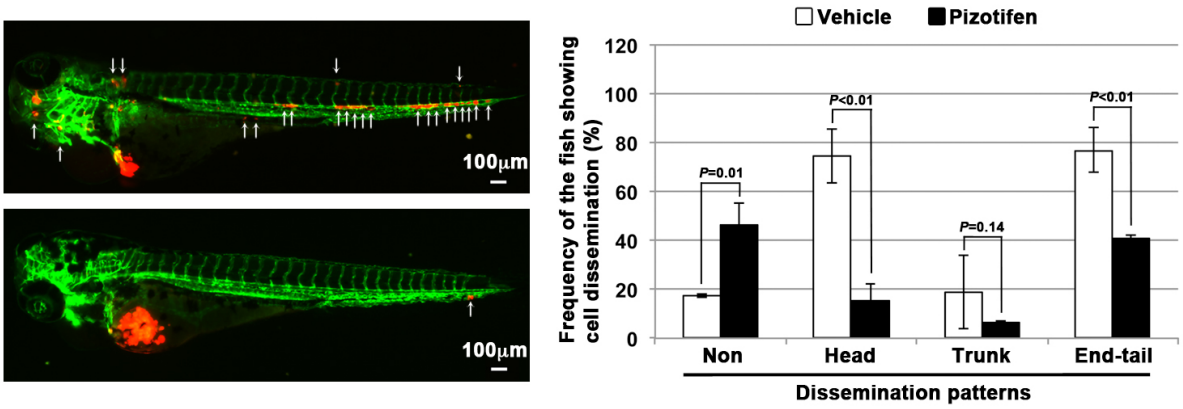

680

681 **Figure S3. Pizotifen suppressed metastatic dissemination of human pancreatic**

682 **cancer cells in a zebrafish xenotransplantation model.**

683 Representative images of dissemination of MIA-PaCa2 cells in zebrafish

684 xenotransplantation model. The fish were inoculated with MIA-PaCa2 cells, and treated

685 with either vehicle (top left) or drug (lower left). White arrows heads indicate

686 disseminated MIA-PaCa2 cells. The images were shown in 4x magnification. Scale bar,

687 100μm. The mean frequencies of the fish showing head, trunk, or end-tail dissemination

688 were tabulated (right). Each value is indicated as the mean ± SEM of two independent

689 experiments. Statistical analysis was determined by Student's *t* test.

690

691 **Table S1. A list of the genes that are involved between gastrulation and metastasis**
692 **progression**
693

Genes	Gastrulation Defects	Ref	Effects in Metastasis	Ref
BMP	Convergence and extension	(1)	EMT	(2)
WNT	Convergence and extension	(3)	Migration and Invasion	(4)
FGF	Convergence and extension	(5)	Invision	(6)
EGF	Epiboly	(7)	Migration	(8)
PDGF	Convergence and extension	(9)	EMT	(10)
CXCL12	Migration of endodermal cells	(11)	Migration and Invasion	(12)
CXCR4	Migration of endodermal cells	(11)	Migration and Invasion	(12)
PIK3CA	Convergence and extension	(13)	Migration and Invasion	(14)
YES	Epiboly	(15)	Migration	(16)
FYN	Epiboly	(17)	Migration and Invasion	(18)
MAPK1	Epiboly	(19)	Migration	(20)
SHP2	Convergence and extension	(21)	Migration	(22)
SNAI1	Convergence and extension	(23)	EMT	(24)
SNAI2	Mesoderm & Neural crest formation	(25)	EMT	(95)
TWIST1	Mesoderm formation	(26)	EMT	(27)
TBXT	Convergence and extension	(3)	EMT	(28)
ZEB1	Epiboly	(29)	EMT	(30)
GSC	Mesodermal patterning	(31)	EMT	(32)
FOXC2	Unclear, defects in gastrulation	(33)	EMT	(34)
STAT3	Convergence and extension	(35)	Migration	(36)
POU5F1	Epiboly	(37)	EMT	(38)
EZH2	Unclear, defects in gastrulation	(39)	Invasion	(40)
EHMT2	Defects in Neurogenesis	(41)	Migration and Invasion	(42)
BMI1	Defects in skelton formation	(43)	EMT	(44)
RHOA	Convergence and extension	(45)	Migration and Invasion	(46)
CDC42	Convergence and extension	(47)	Migration and Invasion	(48)
RAC1	Convergence and extension	(49)	Migration and Invasion	(50)
ROCK2	Convergence and extension	(51)	Migration and Invasion	(52)
PAR1	Convergence and extension	(53)	Migration	(54)
PRKCI	Convergence and extension	(53)	EMT	(55)
CAP1	Convergence and extension	(56)	Migration	(57)
EZR	Epiboly	(58)	Migration	(59)
EPCAM	Epiboly	(60)	Migration and Invasion	(61)
ITGB1 / ITA5	Mesodermal Migration	(62)	Migration and Invasion	(63)
FN1	Convergence and extension	(64)	Invasion	(65)
HAS2	Dorsal migration of lateral cells	(66)	Invasion	(67)
MMP14	Convergence and extension	(68)	Invasion	(69)
COX1	Epiboly	(70)	Invasion	(71)
PTGES	Convergence and extension	(72)	Invasion	(73)
SLC39A6	Aterior migration	(74)	EMT	(75)
GNA12 / 13	Convergence and extension	(41)	Migration and Invasion	(76)
OGT	Epiboly	(77)	Migration and Invasion	(78)
CCN1	Cell Movement	(79)	Migration and Invasion	(80)
TRPM7	Convergence and extension	(81)	Migration	(82)
MAPKAPK2	Epiboly	(83)	Migration	(84)
B4GALT1	Convergence and extension	(85)	Invasion	(86)
IER2	Convergence and extension	(87)	Migration	(88)
TIP1	Convergence and extension	(89)	Migration and Invasion	(90)
PAK5	Convergence and extension	(91)	Migration	(92)
MARCKS	Convergence and extension	(93)	Migration and Invasion	(94)

694

695 **Table S1.**

696 A list of the fifty genes that play essential role in governing both metastasis and

697 gastrulation progression. The gastrulation defects in Xenopus or zebrafish that are

698 induced by knockdown of each of these genes, were indicated. The molecular mechanism

699 in metastasis that are inhibited by knockdown of each of the same genes, were indicated.

700 **Table S2. A list of the drugs that interfere with epiboly progression in zebrafish**
701

Chemical name	Chemical formula	Effect of 10uM	Effect of 50uM
Acitretin	C21H26O3	Delayed	Delayed
Adrenosterone	C19H24O3	Delayed	Delayed
Albendazole	C12H15N3O2S	Severe delayed	Severe delayed
Alfadolone acetate	C23H34O5	Delayed	Delayed
Alfaxalone	C21H32O3	Delayed	Delayed
Alprostadil	C20H34O5	Delayed	Delayed
Altrenogest	C21H26O2	Slightly delayed	Delayed
Ampiroxicam	C20H21N3O7S	Non effect	Delayed
Anethole-trithione	C10H8OS3	Delayed	Delayed
Antimycin A	C28H40N2O9	Delayed	Delayed
Avobenzone	C20H22O3	Delayed	Delayed
Benzoxiquine	C16H11NO2	Non effect	Delayed
Bosentan	C27H29N5O6S	Delayed	Delayed
Butoconazole nitrate	C19H18Cl3N3O3S	Delayed	Toxic lethal
Camptothecine (S,+)	C20H16N2O4	Severe delayed	Severe delayed
Carbenoxolone disodium salt	C34H48Na2O7	Delayed	Toxic lethal
Carmofur	C11H16FN3O3	Slightly delayed	Delayed
Carprofen	C15H12ClNO2	Severe delayed	Toxic lethal
Cefdinir	C14H13N5O5S2	Delayed	Delayed
Celecoxib	C17H14F3N3O2S	Delayed	Delayed
Chlorambucil	C14H19Cl2NO2	Slightly delayed	Delayed
Chlorhexidine	C22H30Cl2N10	Non effect	Toxic lethal
Ciclopirox ethanolamine	C14H24N2O3	Delayed	Severe delayed
Cinoxacin	C12H10N2O5	Delayed	Severe delayed
Clofibrate	C12H15ClO3	Non effect	Severe delayed
Clopidogrel	C16H16ClNO2S	Non effect	Delayed
Clorgyline hydrochloride	C13H16Cl3NO	Delayed	Delayed
Colchicine	C22H25NO6	Non effect	Delayed
Deptropine citrate	C29H35NO8	Delayed	Delayed
Desipramine hydrochloride	C18H23ClN2	Delayed	Delayed
Diclofenac sodium	C14H10Cl2NNaO2	Delayed	Severe delayed
Dicumarol	C19H12O6	Delayed	Severe delayed
Diethylstilbestrol	C18H20O2	Delayed	Toxic lethal
Dimaprit dihydrochloride	C6H17Cl2N3S	Slightly delayed	Delayed
Disulfiram	C10H20N2S4	Delayed	Delayed
Dopamine hydrochloride	C8H12ClNO2	Delayed	Delayed
Eburnamonine (-)	C19H22N2O	Delayed	Delayed
Ethaverine hydrochloride	C24H30ClNO4	Delayed	Delayed
Ethinylestradiol	C20H24O2	Delayed	Severe delayed
Ethopropazine hydrochloride	C19H25ClN2S	Delayed	Delayed
Ethoxyquin	C14H19NO	Non effect	Delayed
Exemestane	C20H24O2	Slightly delayed	Delayed
Ezetimibe	C24H21F2NO3	Slightly delayed	Delayed
Fenbendazole	C15H13N3O2S	Non effect	Delayed
Fenoprofen calcium salt dihydrate	C30H30CaO8	Slightly delayed	Delayed
Fentiazac	C17H12ClNO2S	Toxic lethal	Toxic lethal
Floxuridine	C9H11FN2O5	Delayed	Toxic lethal
Flunixin meglumine	C21H28F3N3O7	Delayed	Toxic lethal
Flutamide	C11H11F3N2O3	Delayed	Toxic lethal
Fluticasone propionate	C25H31F3O5S	Non effect	Delayed
Furosemide	C12H11ClN2O5S	Delayed	Delayed
Gatifloxacin	C19H22FN3O4	Delayed	Delayed
Gemcitabine	C9H11F2N3O4	Delayed	Delayed
Gemfibrozil	C15H22O3	Delayed	Toxic lethal
Gestrinone	C21H24O2	Delayed	Delayed
Haloprogin	C9H4Cl3IO	Delayed	Toxic lethal
Hexachlorophene	C13H6Cl6O2	Delayed	Severe delayed
Hexestrol	C18H22O2	Slightly delayed	Delayed
Ibudilast	C14H18N2O	Non effect	Delayed
Idazoxan hydrochloride	C11H13ClN2O2	Slightly delayed	Delayed
Idazoxan hydrochloride	C11H13ClN2O2	Non effect	Delayed
Idebenone	C19H30O5	Severe delayed	Toxic lethal

Indomethacin	C19H16ClNO4	Non effect	Delayed
Ipriflavone	C18H16O3	Delayed	Severe delayed
Isotretinoin	C20H28O2	Non effect	Severe delayed
Isradipine	C19H21N3O5	Non effect	Delayed
Lansoprazole	C16H14F3N3O2S	Slightly delayed	Delayed
Latanoprost	C26H40O5	Non effect	Delayed
Leflunomide	C12H9F3N2O2	Delayed	Severe delayed
Letrozole	C17H11N5	Non effect	Delayed
Lithocholic acid	C24H40O3	Non effect	Delayed
Lodoxamide	C11H6ClN3O6	Non effect	Delayed
Lofepramine	C26H27ClN2O	Non effect	Delayed
Loratadine	C22H23ClN2O2	Delayed	Delayed
Loxapine succinate	C22H24ClN3O5	Delayed	Delayed
Mebendazole	C16H13N3O3	Severe delayed	Severe delayed
Mebendazole	C22H26N2O2	Non effect	Delayed
Meloxicam	C14H13N3O4S2	Delayed	Toxic lethal
Methiazole	C12H15N3O2S	Delayed	Delayed
Mevastatin	C23H34O5	Non effect	Delayed
MK 801 hydrogen maleate	C20H19NO4	Slightly delayed	Delayed
Nabumetone	C15H16O2	Non effect	Severe delayed
Naftopidil dihydrochloride	C24H30Cl2N2O3	Slightly delayed	Delayed
Nandrolone	C18H26O2	Delayed	Delayed
Naproxen sodium salt	C14H13NaO3	Delayed	Delayed
Niclosamide	C13H8Cl2N2O4	Delayed	Delayed
Nifekalant	C19H27N5O5	Delayed	Delayed
Niflumic acid	C13H9F3N2O2	Delayed	Delayed
Nimesulide	C13H12N2O5S	Non effect	Delayed
Nisoldipine	C20H24N2O6	Delayed	Toxic lethal
Nitazoxanide	C12H9N3O5S	Severe delayed	Severe delayed
Norethindrone	C20H26O2	Non effect	Delayed
Norgestimate	C23H31NO3	Slightly delayed	Delayed
Oxfendazol	C15H13N3O3S	Slightly delayed	Delayed
Oxibendazol	C12H15N3O3	Severe delayed	Severe delayed
Oxymetholone	C21H32O3	Slightly delayed	Delayed
Parbendazole	C13H17N3O2	Severe delayed	Severe delayed
Parthenolide	C15H20O3	Non effect	Delayed
Penciclovir	C10H15N5O3	Non effect	Delayed
Pentobarbital	C11H18N2O3	Non effect	Delayed
Phenazopyridine hydrochloride	C11H12ClN5	Delayed	Toxic lethal
Phenothiazine	C12H9NS	Non effect	Delayed
Phenoxybenzamine hydrochloride	C18H23Cl2NO	Non effect	Delayed
Pizotifen malate	C23H27NO5S	Delayed	Severe delayed
Pramoxine hydrochloride	C17H28ClNO3	Slightly delayed	Delayed
Prilocaine hydrochloride	C13H21ClN2O	Non effect	Delayed
Primidone	C12H14N2O2	Slightly delayed	Delayed
Racecadotril	C21H23NO4S	Slightly delayed	Delayed
Riluzole hydrochloride	C8H6ClF3N2OS	Non effect	Delayed
Ritonavir	C37H48N6O5S2	Non effect	Severe delayed
S(-)Eticlopride hydrochloride	C17H26Cl2N2O3	Delayed	Delayed
Salmeterol	C25H37NO4	Non effect	Delayed
Streptomycin sulfate	C42H84N14O36S3	Non effect	Delayed
Sulconazole nitrate	C18H16Cl3N3O3S	Delayed	Delayed
Tegafur	C8H9FN2O3	Delayed	Delayed
Telmisartan	C33H30N4O2	Severe delayed	Toxic lethal
Tenatoprazole	C16H18N4O3S	Non effect	Delayed
Terbinafine	C21H25N	Non effect	Delayed
Thimerosal	C9H9HgNaO2S	Non effect	Delayed
Thiorphan	C12H15NO3S	Delayed	Delayed
Tolcapone	C14H11NO5	Severe delayed	Severe delayed
Topotecan	C23H23N3O5	Delayed	Delayed
Tracazolate hydrochloride	C16H25ClN4O2	Severe delayed	Delayed
Tribenoside	C29H34O6	Delayed	Delayed
Triclabendazole	C14H9Cl3N2OS	Delayed	Delayed
Triclosan	C12H7Cl3O2	Delayed	Severe delayed
Trioxsalen	C14H12O3	Delayed	Delayed

Troglitazone	C24H27NO5S	Severe delayed	Toxic lethal
Valproic acid	C8H16O2	Non effect	Delayed
Voriconazole	C16H14F3N5O	Non effect	Delayed
Zardaverine	C12H10F2N2O3	Slightly delayed	Delayed
Zuclopenthixol dihydrochloride	C22H27Cl3N2OS	Delayed	Delayed

Table S2. A list of the drugs that interfere with epiboly progression in zebrafish.

A list of positive "hit" drugs that interfered with epiboly progression. Gastrulation defects or status of each of the zebrafish embryos that were treated with either 10μM or 50μM concentrations, are indicated.

References for Table S1.

1. Kondo M (2007) Bone morphogenetic proteins in the early development of zebrafish. *FEBS J* 274(12):2960-2967.
2. Katsuno Y, *et al.* (2008) Bone morphogenetic protein signaling enhances invasion and bone metastasis of breast cancer cells through Smad pathway. *Oncogene* 27(49):6322-6333.
3. Tada M & Smith JC (2000) Xwnt11 is a target of Xenopus Brachyury: regulation of gastrulation movements via Dishevelled, but not through the canonical Wnt pathway. *Development* 127:2227-2238.
4. Vincan E & Barker N (2008) The upstream components of the Wnt signalling pathway in the dynamic EMT and MET associated with colorectal cancer progression. *Clin Exp Metastasis* 25(6):657-663.
5. Yang X, Dormann D, Munsterberg AE, & Weijer CJ (2002) Cell movement patterns during gastrulation in the chick are controlled by positive and negative chemotaxis mediated by FGF4 and FGF8. *Dev Cell* 3(3):425-437.
6. Nomura S, *et al.* (2008) FGF10/FGFR2 signal induces cell migration and invasion in pancreatic cancer. *Br J Cancer* 99(2):305-313.
7. Song S, *et al.* (2013) Pou5f1-dependent EGF expression controls E-cadherin endocytosis, cell adhesion, and zebrafish epiboly movements. *Dev Cell* 24(5):486-501.
8. Lu Z, Jiang G, Blume-Jensen P, & Hunter T (2001) Epidermal growth factor-induced tumor cell invasion and metastasis initiated by dephosphorylation and downregulation of focal adhesion kinase. *Mol Cell Biol* 21(12):4016-4031.
9. Damm EW & Winklbauer R (2011) PDGF-A controls mesoderm cell orientation and radial intercalation during Xenopus gastrulation. *Development* 138(3):565-575.
10. Jechlinger M, *et al.* (2006) Autocrine PDGFR signaling promotes mammary cancer metastasis. *J Clin Invest* 116(6):1561-1570.
11. Mizoguchi T, Verkade H, Heath JK, Kuroiwa A, & Kikuchi Y (2008) Sdf1/Cxcr4 signaling controls the dorsal migration of endodermal cells during zebrafish gastrulation. *Development* 135(15):2521-2529.
12. Shen HB, Gu ZQ, Jian K, & Qi J (2013) CXCR4-mediated Stat3 activation is essential for CXCL12-induced cell invasion in bladder cancer. *Tumour Biol* 34(3):1839-1845.
13. Montero J-A, Kilian B, Chan J, Bayliss PE, & Heisenberg C-P (2003) Phosphoinositide 3-Kinase Is Required for Process Outgrowth and Cell

744 Polarization of Gastrulating Mesendodermal Cells. *Current Biology*
745 13(15):1279-1289.
746 14. Wander SA*, et al.* (2013) PI3K/mTOR inhibition can impair tumor invasion
747 and metastasis in vivo despite a lack of antiproliferative action in vitro:
748 implications for targeted therapy. *Breast Cancer Res Treat* 138(2):369-381.
749 15. Tsai WB, Zhang X, Sharma D, Wu W, & Kinsey WH (2005) Role of Yes kinase
750 during early zebrafish development. *Dev Biol* 277(1):129-141.
751 16. Barraclough J, Hodgkinson C, Hogg A, Dive C, & Welman A (2007) Increases in
752 c-Yes Expression Level and Activity Promote Motility But Not Proliferation of
753 Human Colorectal Carcinoma Cells. *Neoplasia* 9(9):745-IN732.
754 17. Sharma D, Holets L, Zhang X, & Kinsey WH (2005) Role of Fyn kinase in
755 signaling associated with epiboly during zebrafish development. *Dev Biol*
756 285(2):462-476.
757 18. Yadav V & Denning MF (2011) Fyn is induced by Ras/PI3K/Akt signaling and
758 is required for enhanced invasion/migration. *Mol Carcinog* 50(5):346-352.
759 19. Krens SF*, et al.* (2008) Distinct functions for ERK1 and ERK2 in cell migration
760 processes during zebrafish gastrulation. *Dev Biol* 319(2):370-383.
761 20. Radtke S, Milanovic M, & Rossé C (2013) ERK2 but not ERK1 mediates HGF-
762 induced motility in non-small cell lung carcinoma cell lines. *J Cell Sci.*
763 126(Pt11):2381-2391.
764 21. Jopling C, van Geemen D, & den Hertog J (2007) Shp2 knockdown and
765 Noonan/LEOPARD mutant Shp2-induced gastrulation defects. *PLoS Genet*
766 3(12):e225.
767 22. Wang FM*, et al.* (2005) SHP-2 promoting migration and metastasis of MCF-7
768 with loss of E-cadherin, dephosphorylation of FAK and secretion of MMP-9
769 induced by IL-1beta in vivo and in vitro. *Breast Cancer Res Treat* 89(1):5-14.
770 23. Ip YT & Gridley T (2002) Cell movements during gastrulation: snail
771 dependent and independent pathways. *Curr Opin Genet Dev* 12(4):423-429.
772 24. Batlle E, Sancho E, Francí C, Domínguez D, & Monfar M (2000) The
773 transcription factor snail is a repressor of E-cadherin gene expression in
774 epithelial tumour cells. *Nat Cell Biol* 2(2):84-89.
775 25. Shi J, Severson C, Yang J, Wedlich D, & Klymkowsky MW (2011) Snail2
776 controls mesodermal BMP/Wnt induction of neural crest. *Development*
777 138(15):3135-3145.
778 26. Castanon I & Baylies MK (2002) A Twist in fate: evolutionary comparison of
779 Twist structure and function. *Gene* 287(1-2):11-22.
780 27. Yang J*, et al.* (2004) Twist, a master regulator of morphogenesis, plays an
781 essential role in tumor metastasis. *Cell* 117(7):927-939.
782 28. Fernando RI*, et al.* (2010) The T-box transcription factor Brachyury
783 promotes epithelial-mesenchymal transition in human tumor cells. *J Clin*
784 *Invest* 120(2):533-544.
785 29. Vannier C, Mock K, Brabletz T, & Driever W (2013) Zeb1 regulates E-cadherin
786 and Epcam (epithelial cell adhesion molecule) expression to control cell
787 behavior in early zebrafish development. *J Biol Chem* 288(26):18643-18659.
788 30. Spaderna S*, et al.* (2008) The transcriptional repressor ZEB1 promotes
789 metastasis and loss of cell polarity in cancer. *Cancer Res* 68(2):537-544.
790 31. Sander V, Reversade B, & De Robertis EM (2007) The opposing homeobox
791 genes Goosecoid and Vent1/2 self-regulate Xenopus patterning. *EMBO J*
792 26(12):2955-2965.
793 32. Hartwell KA*, et al.* (2006) The Spemann organizer gene, Goosecoid, promotes
794 tumor metastasis. *Proc Natl Acad Sci U S A* 103(50):18969-18974.

795 33. Wilm B, James RG, Schultheiss TM, & Hogan BL (2004) The forkhead genes,
796 Foxc1 and Foxc2, regulate paraxial versus intermediate mesoderm cell fate.
797 *Dev Biol* 271(1):176-189.
798 34. Mani SA, *et al.* (2007) Mesenchyme Forkhead 1 (FOXC2) plays a key role in
799 metastasis and is associated with aggressive basal-like breast cancers. *Proc*
800 *Natl Acad Sci U S A* 104(24):10069-10074.
801 35. Miyagi C, *et al.* (2004) STAT3 noncell-autonomously controls planar cell
802 polarity during zebrafish convergence and extension. *J Cell Biol* 166(7):975-
803 981.
804 36. Abdulghani J, *et al.* (2008) Stat3 promotes metastatic progression of prostate
805 cancer. *Am J Pathol* 172(6):1717-1728.
806 37. Lachnit M, Kur E, & Driever W (2008) Alterations of the cytoskeleton in all
807 three embryonic lineages contribute to the epiboly defect of Pou5f1/Oct4
808 deficient MZspg zebrafish embryos. *Dev Biol* 315(1):1-17.
809 38. Dai X, *et al.* (2013) OCT4 regulates epithelial-mesenchymal transition and its
810 knockdown inhibits colorectal cancer cell migration and invasion. *Oncol Rep*
811 29(1):155-160.
812 39. O'Carroll D, *et al.* (2001) The polycomb-group gene Ezh2 is required for early
813 mouse development. *Mol Cell Biol* 21(13):4330-4336.
814 40. Ren G, *et al.* (2012) Polycomb protein EZH2 regulates tumor invasion via the
815 transcriptional repression of the metastasis suppressor RKIP in breast and
816 prostate cancer. *Cancer Res* 72(12):3091-3104.
817 41. Lin F, *et al.* (2005) Essential roles of G{alpha}12/13 signaling in distinct cell
818 behaviors driving zebrafish convergence and extension gastrulation
819 movements. *J Cell Biol* 169(5):777-787.
820 42. Chen MW, *et al.* (2010) H3K9 histone methyltransferase G9a promotes lung
821 cancer invasion and metastasis by silencing the cell adhesion molecule Ep-
822 CAM. *Cancer Res* 70(20):7830-7840.
823 43. van der Lugt NM, *et al.* (1994) Posterior transformation, neurological
824 abnormalities, and severe hematopoietic defects in mice with a targeted
825 deletion of the bmi-1 proto-oncogene. *Genes Dev* 8(7):757-769.
826 44. Guo BH, *et al.* (2011) Bmi-1 promotes invasion and metastasis, and its
827 elevated expression is correlated with an advanced stage of breast cancer.
828 *Mol Cancer* 10(1):10.
829 45. Zhu S, Liu L, Korzh V, Gong Z, & Low BC (2006) RhoA acts downstream of
830 Wnt5 and Wnt11 to regulate convergence and extension movements by
831 involving effectors Rho kinase and Diaphanous: use of zebrafish as an in vivo
832 model for GTPase signaling. *Cell Signal* 18(3):359-372.
833 46. Yoshioka K, Nakamori S, & Itoh K (1999) Overexpression of small GTP-
834 binding protein RhoA promotes invasion of tumor cells. *Cancer Res*
835 59(8):2004-2010.
836 47. Choi SC & Han JK (2002) Xenopus Cdc42 regulates convergent extension
837 movements during gastrulation through Wnt/Ca2+ signaling pathway. *Dev*
838 *Biol* 244(2):342-357.
839 48. Reymond N, *et al.* (2012) Cdc42 promotes transendothelial migration of
840 cancer cells through beta1 integrin. *J Cell Biol* 199(4):653-668.
841 49. Habas R, Dawid IB, & He X (2003) Coactivation of Rac and Rho by
842 Wnt/Frizzled signaling is required for vertebrate gastrulation. . *Genes Dev*
843 17(2):295-309.
844 50. Vega FM & Ridley AJ (2008) Rho GTPases in cancer cell biology. *FEBS Lett*
845 582(14):2093-2101.

846 51. Marlow F, Topczewski J, Sepich D, & Solnica-Krezel L (2002) Zebrafish Rho
847 kinase 2 acts downstream of Wnt11 to mediate cell polarity and effective
848 convergence and extension movements. *Curr Biol* 12(11):876-884.
849 52. Itoh K, *et al.* (1999) An essential part for Rho-associated kinase in the
850 transcellular invasion of tumor cells. *Nat Med* 5(2):221-225.
851 53. Kusakabe M & Nishida E (2004) The polarity-inducing kinase Par-1 controls
852 Xenopus gastrulation in cooperation with 14-3-3 and aPKC. *EMBO J*
853 23(21):4190-4201.
854 54. Shi X, Gangadharan B, Brass LF, Ruf W, & Mueller BM (2004) Protease-
855 activated receptors (PAR1 and PAR2) contribute to tumor cell motility and
856 metastasis. *Mol Cancer Res* 2(7):395-402.
857 55. Gunaratne A, Thai BL, & Di Guglielmo GM (2013) Atypical protein kinase C
858 phosphorylates Par6 and facilitates transforming growth factor beta-induced
859 epithelial-to-mesenchymal transition. *Mol Cell Biol* 33(5):874-886.
860 56. Seifert K, Ibrahim H, Stodtmeister T, Winklbauer R, & Niessen CM (2009) An
861 adhesion-independent, aPKC-dependent function for cadherins in
862 morphogenetic movements. *J Cell Sci* 122(Pt 14):2514-2523.
863 57. Yamazaki K, *et al.* (2009) Adenylate cyclase-associated protein 1
864 overexpressed in pancreatic cancers is involved in cancer cell motility. *Lab*
865 *Invest* 89(4):425-432.
866 58. Link V, *et al.* (2006) Identification of regulators of germ layer morphogenesis
867 using proteomics in zebrafish. *J Cell Sci* 119(Pt 10):2073-2083.
868 59. Khanna C, *et al.* (2004) The membrane-cytoskeleton linker ezrin is necessary
869 for osteosarcoma metastasis. *Nat Med* 10(2):182-186.
870 60. Slanchev K, *et al.* (2009) The epithelial cell adhesion molecule EpCAM is
871 required for epithelial morphogenesis and integrity during zebrafish epiboly
872 and skin development. *PLoS Genet* 5(7):e1000563.
873 61. Ni J, *et al.* (2012) Role of the EpCAM (CD326) in prostate cancer metastasis
874 and progression. *Cancer Metastasis Rev* 31(3-4):779-791.
875 62. Skalski M, Alfandari D, & Darribere T (1998) A key function for alphav
876 containing integrins in mesodermal cell migration during Pleurodeles waltl
877 gastrulation. *Dev Biol* 195(2):158-173.
878 63. Felding-Habermann B (2003) Integrin adhesion receptors in tumor
879 metastasis. *Clin Exp Metastasis* 20(3):203-213.
880 64. Marsden M & DeSimone DW (2003) Integrin-ECM Interactions Regulate
881 Cadherin-Dependent Cell Adhesion and Are Required for Convergent
882 Extension in Xenopus. *Current Biology* 13(14):1182-1191.
883 65. Malik G, *et al.* (2010) Plasma fibronectin promotes lung metastasis by
884 contributions to fibrin clots and tumor cell invasion. *Cancer Res* 70(11):4327-
885 4334.
886 66. Bakkers J, *et al.* (2004) Has2 is required upstream of Rac1 to govern dorsal
887 migration of lateral cells during zebrafish gastrulation. *Development*
888 131(3):525-537.
889 67. Kim HR, *et al.* (2004) Hyaluronan facilitates invasion of colon carcinoma cells
890 in vitro via interaction with CD44. *Cancer Res* 64(13):4569-4576.
891 68. Coyle RC, Latimer A, & Jessen JR (2008) Membrane-type 1 matrix
892 metalloproteinase regulates cell migration during zebrafish gastrulation:
893 evidence for an interaction with non-canonical Wnt signaling. *Exp Cell Res*
894 314(10):2150-2162.
895 69. Perentes JY, *et al.* (2011) Cancer cell-associated MT1-MMP promotes blood
896 vessel invasion and distant metastasis in triple-negative mammary tumors.
897 *Cancer Res* 71(13):4527-4538.

898 70. Cha YI, *et al.* (2006) Cyclooxygenase-1-derived PGE2 promotes cell motility
899 via the G-protein-coupled EP4 receptor during vertebrate gastrulation. *Genes*
900 *Dev* 20(1):77-86.
901 71. Kundu N & Fulton AM (2002) Selective cyclooxygenase (COX)-1 or COX-2
902 inhibitors control metastatic disease in a murine model of breast cancer.
903 *Cancer Res* 62(8):2343-2346.
904 72. Speirs CK, *et al.* (2010) Prostaglandin Gbetagamma signaling stimulates
905 gastrulation movements by limiting cell adhesion through Snai1a
906 stabilization. *Development* 137(8):1327-1337.
907 73. Wang D & Dubois RN (2006) Prostaglandins and cancer. *Gut* 55(1):115-122.
908 74. Yamashita S, *et al.* (2004) Zinc transporter LIVI controls epithelial-
909 mesenchymal transition in zebrafish gastrula organizer. *Nature*
910 429(6989):298-302.
911 75. Lue HW, *et al.* (2011) LIV-1 promotes prostate cancer epithelial-to-
912 mesenchymal transition and metastasis through HB-EGF shedding and EGFR-
913 mediated ERK signaling. *PLoS One* 6(11):e27720.
914 76. Yagi H, *et al.* (2011) A synthetic biology approach reveals a CXCR4-G13-Rho
915 signaling axis driving transendothelial migration of metastatic breast cancer
916 cells. *Sci Signal* 4(191):ra60.
917 77. Webster DM, *et al.* (2009) O-GlcNAc modifications regulate cell survival and
918 epiboly during zebrafish development. *BMC Dev Biol* 9:28.
919 78. Lynch TP, *et al.* (2012) Critical role of O-Linked beta-N-acetylglucosamine
920 transferase in prostate cancer invasion, angiogenesis, and metastasis. *J Biol*
921 *Chem* 287(14):11070-11081.
922 79. Latinkic BV (2003) Xenopus Cyr61 regulates gastrulation movements and
923 modulates Wnt signalling. *Development* 130(11):2429-2441.
924 80. Lin J, *et al.* (2012) A novel anti-Cyr61 antibody inhibits breast cancer growth
925 and metastasis in vivo. *Cancer Immunol Immunother* 61(5):677-687.
926 81. Liu W, *et al.* (2011) TRPM7 regulates gastrulation during vertebrate
927 embryogenesis. *Dev Biol* 350(2):348-357.
928 82. Middelbeek J, *et al.* (2012) TRPM7 is required for breast tumor cell
929 metastasis. *Cancer Res* 72(16):4250-4261.
930 83. Holloway BA, *et al.* (2009) A novel role for MAPKAPK2 in morphogenesis
931 during zebrafish development. *PLoS Genet* 5(3):e1000413.
932 84. Kumar B, *et al.* (2010) p38 mitogen-activated protein kinase-driven
933 MAPKAPK2 regulates invasion of bladder cancer by modulation of MMP-2
934 and MMP-9 activity. *Cancer Res* 70(2):832-841.
935 85. Machingo QJ, Fritz A, & Shur BD (2006) A beta1,4-galactosyltransferase is
936 required for convergent extension movements in zebrafish. *Dev Biol*
937 297(2):471-482.
938 86. Zhu X, *et al.* (2005) Elevated beta1,4-galactosyltransferase I in highly
939 metastatic human lung cancer cells. Identification of E1AF as important
940 transcription activator. *J Biol Chem* 280(13):12503-12516.
941 87. Hong SK, Tanegashima K, & Dawid IB (2011) XIer2 is required for convergent
942 extension movements during Xenopus development. *Int J Dev Biol* 55(10-
943 12):917-921.
944 88. Neeb A, *et al.* (2012) The immediate early gene Ier2 promotes tumor cell
945 motility and metastasis, and predicts poor survival of colorectal cancer
946 patients. *Oncogene* 31(33):3796-3806.
947 89. Besser J, Leito JT, van der Meer DL, & Bagowski CP (2007) Tip-1 induces
948 filopodia growth and is important for gastrulation movements during
949 zebrafish development. *Dev Growth Differ* 49(3):205-214.

950 90. Han M, Wang H, Zhang HT, & Han Z (2012) The PDZ protein TIP-1 facilitates
951 cell migration and pulmonary metastasis of human invasive breast cancer
952 cells in athymic mice. *Biochem Biophys Res Commun* 422(1):139-145.
953 91. Faure S, *et al.* (2005) Xenopus p21-activated kinase 5 regulates blastomeres'
954 adhesive properties during convergent extension movements. *Dev Biol*
955 277(2):472-492.
956 92. Gong W, *et al.* (2009) P21-activated kinase 5 is overexpressed during
957 colorectal cancer progression and regulates colorectal carcinoma cell
958 adhesion and migration. *Int J Cancer* 125(3):548-555.
959 93. Iioka H, Ueno N, & Kinoshita N (2004) Essential role of MARCKS in cortical
960 actin dynamics during gastrulation movements. *J Cell Biol* 164(2):169-174.
961 94. Rombouts K, *et al.* (2013) Myristoylated Alanine-Rich protein Kinase C
962 Substrate (MARCKS) expression modulates the metastatic phenotype in
963 human and murine colon carcinoma in vitro and in vivo. *Cancer Lett*
964 333(2):244-252.
965 95. Medici D, Hay ED, & B.R. O (2008) Snail and Slug Promote Epithelial-
966 Mesenchymal Transition through -Catenin–T-Cell Factor-4-dependent Expression of
967 Transforming Growth Factor-3. Molecular Biology of the Cell 19(11):4875–4887.